2011

Analyses of Variable Refrigerant Flow and Exergy in Air Conditioning Systems

Rashid Ali Alshatti
University of South Florida, q8_r@hotmail.com

Analyses of Variable Refrigerant Flow and Exergy in Air Conditioning Systems

by

Rashid Ali Alshatti

A thesis submitted in partial fulfillment
of the requirements for the degree of
Master of Science
Department of Mechanical Engineering
College of Engineering
University of South Florida

Major Professor: Muhammad M. Rahman, Ph.D.
Luis Rosario, Ph.D.
Frank Pyrtle, III, Ph.D.
Kamal Alsharif, Ph.D.

Date of Approval:
October 12, 2011

Keywords: COP, Refrigeration, Simulation, Efficiency, Dead State

Dedication

To God, the Beneficent, the Merciful.

To my father, mother, brothers, and sisters.

To my Major Professor Muhammad M. Rahman.

Finally, to all of my friends in the United States and Kuwait.

Acknowledgements

I would like to thank my colleagues Ammar Bahman and Mutasim Elsheikh for their help and support during my course of study. I would like to also thank Dr. Luis Rosario and Dr. Jorge C. Lallave for their guidance and support. Finally, I would like to thank all of the committee members who dedicated their time and effort to review this work.

Table of Contents

List of Tables

List of Figures

List of Symbols

Texts

COP	Coefficient of performance
T	Temperature [°C]
RH	Relative humidity
q	Volumetric flow rate [m^3/s]
Q	Heat transfer rate [kW]
W	Work rate [kW]
m	Mass flow rate [kg/s]
h	Specific enthalpy [kJ/kg]
PLR	Part load ratio
Pc	Power consumption [kW]
PLF	Part load factor
P	Pressure [kPa]
s	Specific entropy [kJ/kg·K]
S_{gen}	Entropy generation rate [kW/K]
Ex	Exergy rate [kW]
SHR	Sensible heat ratio

Greek Symbols

η	Efficiency
ψ	Specific exergy of fluid stream [kJ/kg]

Subscripts

o	Outside
r	Room
m	Mixture
b	Bypass
evap	Evaporator
tot	Total
cond	Condenser
c	Compressor
isen	Isentropic
cyc	Cycle
full	Full load
a	Dry air
w	Water
d	Destruction
dead	Dead state
s	Supply
out	Output
u	Dehumidifier or condensing unit
in	Input

AM	Adiabatic mixing
sys	System
ex	Exergy
sen	Sensible
lat	Latent

Abstract

This thesis consists of two research problems in the air conditioning (A/C) area. For the first problem, the aim is to model and simulate a variable refrigerant flow (VRF) air conditioning system. The coefficient of performance (COP) for refrigeration or heat pump system is one of the critical parameters for designing an air conditioning system. The modeling of the system components for a VRF cycle under different cooling conditions using R-134a and R-22 as refrigerants was carried out. Calculations were performed by varying different parameters such as condenser and evaporator temperatures, and refrigerant type. The R-134a refrigerant shows a better performance when multiple evaporators are present. Part load performance evaluation was also done for both refrigerants. The simulation results compared reasonably well with available experimental data.

In the second problem, the objective is to develop a mathematical model that covers the mass, energy, entropy, and exergy balances of a typical air conditioning system. The model examines how the exergy efficiency of an air conditioning system can be used to measure its performance, bypass configuration, and additional significant environmental factors that affect an A/C system's design. The effects of outside air parameters, room parameters, room sensible and latent heat loads, and dead state properties on exergy efficiency were investigated. The range of parameters covered included outside air temperature (T_o= 25-60^{o}C) and relative humidity (RH_o = 50-85%),

sensible heat load (Q_{sen} = 11.50-13.25 kW), latent heat load (Q_{lat} = 3.00-4.75 kW), room air temperature (T_r= 18-25^oC), and relative humidity (RH_r= 30-44%), and outside-mixture air flow rate ratio (q_o / q_m = 0.21-0.71). Two novel dead state conditions were selected to further analyze their effects on the system. Present exergy results indicate that an A/C system is quite sensitive to air properties, sensible and latent cooling loads, and dead state conditions.

Chapter 1: Introduction

1.1 Literature Review (Variable Refrigerant Flow)

The primary function of all air conditioning systems is to provide thermal comfort for building occupants. There is a wide range of system types available, starting with the basic window-fitted unit to the very latest variable refrigerant flow (VRF) and variable air volume (VAV) equipment. Determining which system best suits the cooling capacity needs will depend on several factors. VRF air conditioning systems, for example, are well known for their high coefficient of performance (COP) which directly contributes to energy cost savings.

There are two basic types of VRF systems: cooling or heating only and energy recovery. Energy recovery systems can simultaneously cool and/or heat different parts of the air conditioned area. Refrigerants R-22 and R-134a are widely used in air conditioning applications. Nowadays, most VRF systems provide cooling and heating using refrigerant R-410a as the working fluid because of its zero potential to environmental impact. The consumption of fossil fuels and the emissions of greenhouse gases associated with energy generation lead to considerable monetary costs and environmental consequences. An alternative solution for this increasing demand of electrical power is the implementation of VRF systems due to its flexibility and high efficiency in comparison with traditional central air conditioning systems.

In general, there is one compressor in each VRF unit. The VRF system capacity can be adjusted by varying the compressor's frequency to match the thermal load condition. The indoor units in a VRF system can be independently controlled by regulating the refrigerant flow rate to meet the cooling or heating requirements in each room. The flexibility of a VRF system is especially suited for a building with different functional rooms and complicated load conditions, such as hospitals, hotels, apartment complexes, and shopping centers. Conventional systems would require several condensing units or additional duct work to reach these same results.

Stoeker and Jones [1] gave an example about the dairy industry where VRF systems are used because one evaporator is required to cool the milk at 2.2°C and a second evaporator freezes the ice cream at -35.0°C. Such systems can be studied and applied to all industrial buildings with multiple cooling zones utilizing a variety of temperature ranges as required. Strand et al. [2] suggested that new HVAC systems development must be simulated and studied through software. Xia et al. [3] experimentally examined the VRF system and measured values of pressure and temperature at different locations of the cycle.

Goetzler [4] discussed the history and applications of VRF systems. They were initially developed in Japan more than two decades ago. Nowadays, approximately half of medium-sized commercial buildings and one-third of large commercial buildings are using VRF systems in Japan [4]. The author suggested that buildings with multiple cooling/heating zones such as multi-story buildings are best fit for a VRF system. The usefulness of the VRF system is its ability to control the flow of refrigerant to each evaporator. This will provide personal comfort in multiple zones even though they are all

connected to one condensing unit. It can also provide cooling in one zone and heating in another zone by transferring the heat removed from the cooling zone to the heating zone. Duct losses which can account for 20% of total airflow can be eliminated by using a VRF system [4].

Zhou et al. [5] compared the VRF system with two conventional air conditioning units. As part of their analysis, the authors found that the VRF unit is the most energy efficient system. They found that the VRF system was 22.2% more efficient than VAV system. Also the VRF unit was 11.7% more energy efficient than the fan-coil plus fresh air (FPFA) system. Zhou et al. [6] simulated and experimentally monitored the variable refrigerant volume (VRV) system on an hourly basis. The authors found that VRV system has higher coefficient of performance than their rating. Aynur et al. [7] compared VRF systems to VAV systems numerically and found that VRF systems can save from 27.1% to 57.9% of energy.

Wang et al. [8] presented a numerical model to calculate the coefficient of performance for a partial load VRF system. Li et al. [9] numerically studied a water-cooled VRF system where water was used to cool the condensing unit instead of air. Most of the simulated data using EnergyPlus was in agreement with the measured data obtained from Dalian, China. Conversely, the measured coefficients of performance (COP) were lower than the simulated ones. Li and Wu [10] found that the heat recovery VRF system can save up to 17% of the energy consumption compared to a heat pump VRF system setup. This heat recovery VRF system offered an additional advantage that it can provide cooling and heating for different zones at the same time. Bettanini et al. [11] developed a mathematical model for calculating the part load performance of an air

conditioning system based on experimental values obtained from laboratory tests. According to the authors, only one full load test and one part load test for the system are required to find the correlations for part load ratio (PLR) and part load factor (PLF).

1.2 Literature Review (Exergy)

The energy needed to process and circulate air in buildings and to control the humidity and temperature has increased continuously during the last decades especially in developing countries. This energy demand was caused by the increase of thermal loads to fulfill occupant comfort demands, climate changes, and architectural trends. Energy and fuel cost savings and air conditioning system optimization are becoming more important in engineering design of psychrometric processes. In the case of an air conditioning system design, generally energy consumption can be minimized by analyzing losses in the system. One tool of analyzing losses is to analyze the exergy efficiency of a system. Exergy or availability of a system represents its maximum work potential at a given state. Therefore, exergy loss is a key factor to evaluate the thermodynamic performance of a system. By doing such an analysis, one can determine the parameters which have greater effect on the system and can be improved.

Krakow [12] discussed the relationships between irreversibility, exergy destruction, and entropy generation for different heat pumps. The author studied how the concepts of irreversibility, exergy destruction, and entropy generation are closely related mathematically and conceptually for the components and complete heat pump system. The author also emphasized that the component's irreversibility has to be related to the entire system's irreversibility. The thermal, mechanical, and chemical exergy of moist air

were examined by Chengqin et al. [13]. The authors showed the results for different evaporative cooling models. In addition, the authors mentioned the importance of the dead state temperature selection in order to simplify the exergy calculation. Cervantes and Torres-Reyes [14] conducted an experimental exergy analysis of solar assisted heat pumps. The authors found that solar assisted heat pumps can be improved by reducing exergy losses in collector evaporator.

The effects of heating and cooling loads on system performance and exergy efficiency were investigated by Bilgen and Takahashi [15]. The authors used experimental data to calculate the coefficient of performance (COP) of the system. They found that the exergy efficiency decreases with the increase of the cooling or heating load. Qureshi and Zubair [16] studied various psychrometric processes by using exergy analysis. Exergy calculations were done for several processes to determine the effect of inlet properties, and their effects on some output parameters and the exergy efficiency of the system. Utlu and Hepbasli [17] presented a study on the necessity of increasing exergy efficiency in residential and commercial buildings. Additionally, the authors indicated the importance of using the natural resources more efficiently to manage the increasing demand for electricity.

The exergy analysis of the air conditioning system for hot and humid climate was conducted by Alpuche et al. [18]. The authors showed hourly exergy efficiency data for different systems and suggested that the exergy analysis can be used for building design purposes. A procedure for estimating the minimum work required for air cooling and dehumidification units was developed by Alhazmy [19]. Rosen et al. [20] showed that the exergy analysis of a system should be done in order to reach sustainability. The exergy

analysis could guide us to understand how much impact the environment has on a system in order to improve its design. Muangnoi et al. [21] applied exergy analysis to a counter flow wet cooling tower. The authors found that the only way to identify the maximum performance of the system was by exergy analysis. Wei and Zmeureanu [22] performed energy and exergy analysis for variable air volume systems. The authors found that the exergy efficiency range was from 2% to 3% and the rest is waste of energy. Ahmad et al. [23] carried out a review of the exergy destruction and efficiency of a vapor compression refrigeration system. As part of the results, the authors found that the exergy of the cycle depends on many factors such as evaporating and condensing temperatures, sub-cooling, compressor power, and dead state temperature. They found that the highest exergy loss occurred in the compressor component of the system. Kanoglu et al. [24] presented the exergy formulation for various psychrometric processes that include simple heating or cooling, evaporative cooling, heating with humidification, cooling with dehumidification, and adiabatic mixing. Their results showed the advantages of using exergy analysis to improve the efficiency of psychrometric processes.

1.3 Objectives

1.3.1 Variable Refrigerant Flow

From the literature review in section 1.1, it can be noticed that even though a number of studies have considered the VRF system, only a few have examined the effects of the condenser and multiple evaporator temperature conditions for different choices of working fluid. Therefore, this study attempted to carry out a comprehensive investigation

of the coefficient of performance (COP) for a variable refrigerant flow air conditioning system under different conditions. This included taking into account the surrounding conditions using a number of refrigerants as the working fluid and both full and part load conditions. Results are presented for both R-134a and R-22. In addition, a comparison was done between current variable refrigerant flow cycle results and a single evaporator cycle results. Finally, a comparison between experimental data from Hitachi and Toshiba catalogs to the current cycle under the same conditions has been done to strengthen and support present results.

1.3.2 Exergy

Although several investigations provided very useful information, only a few attempted to produce an exergy analysis for a group of psychrometric processes that happens in a HVAC system. In addition, none of the studies have considered the integration of the exergy destruction in a room, although it is a very important part of the HVAC system design. These studies only focused on the adiabatic mixing, dehumidification, refrigerant, heat pump, or condensing unit of the system. The objective of the present research is to study a standard air conditioning system through exergy analysis including the condensing unit, room, and environment under several cooling load conditions. The mass, energy, entropy, and exergy balances and exergy efficiency relations for some key air conditioning system processes are included as a part of the mathematical modeling of the system. Two dead state conditions were selected and analyzed. The first dead state temperature selection is equal to the outside temperature. Kanoglu et al. [24] and many others used the dead state temperature as the inlet

temperature of the system. The second dead state temperature selection is equal to the thermodynamic reference temperature as discussed by Moran et al. [25].

Chapter 2: Analysis of a Variable Refrigerant Flow Air Conditioning System

2.1 Mathematical Model

The simulation model was built using CHEMCAD [26], which is a software used for chemical process simulation. The properties of the working fluid were generated within the CHEMCAD software using the Peng Robinson equilibrium and enthalpy model [27]. In order to verify the accuracy of simulated results, hand calculations were done for a sample system using thermodynamic properties linked in Moran et al. [25]. The calculated results showed an excellent agreement with the simulated results obtained from CHEMCAD.

Figure 2.1 shows a schematic of the refrigeration cycle for a variable refrigerant flow air conditioning system. The arrow that is going toward the compressor is the total working fluid feed stream. A refrigerant flow control is used after the condenser to separate the mass flow rate for each evaporator based on each evaporator's temperature and cooling load. The refrigerant flow control is one of the design challenges for the VRF systems and is thoroughly investigated in Kim et al. [28] and others. The masses flowing out of evaporators 1 and 2 enter thermal expansion valves to bring them to the same pressure as evaporator 3 before mixing and reconnecting them to the compressor.

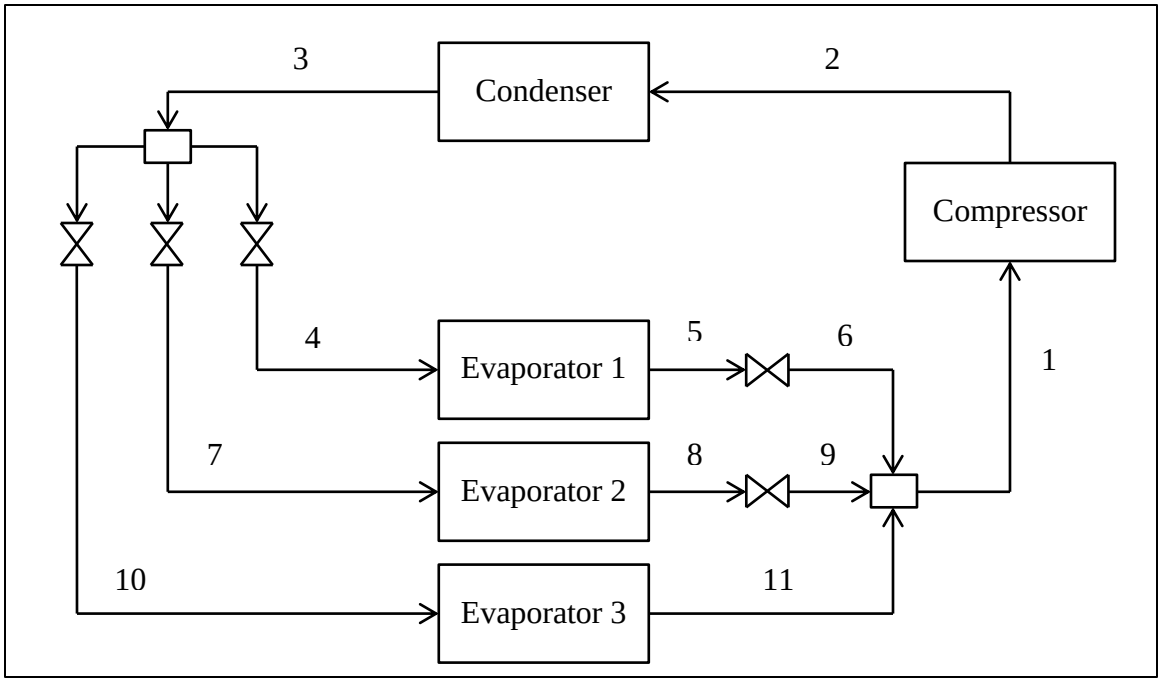

Figure 2.1: Schematic diagram of the variable refrigerant flow refrigeration cycle.

The thermodynamic model was developed by performing mass and energy balance at each component of the system. Figure 2.2 shows the P-h diagram of the cycle which illustrates the behavior of the system at each point.

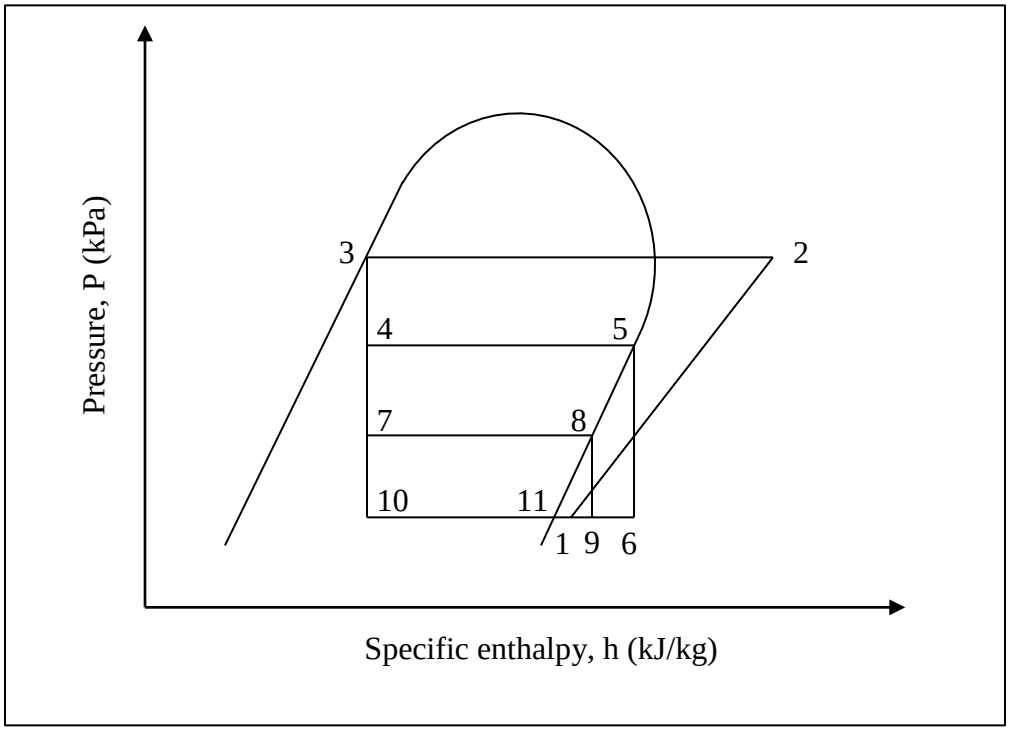

Figure 2.2: Pressure versus specific enthalpy diagram of the cycle.

The mass flow rate for each evaporator can be obtained by an energy balance for each evaporator as follows:

$$m_1 = \frac{Q_{evap1}}{h_5 - h_4} \tag{1}$$

$$m_2 = \frac{Q_{evap2}}{h_8 - h_7} \tag{2}$$

$$m_3 = \frac{Q_{evap3}}{h_{11} - h_{10}} \tag{3}$$

The total mass flow rate can be written as:

$$m_{tot} = m_1 + m_2 + m_3 \tag{4}$$

The enthalpy of the compressor's inlet can be calculated by an energy balance around the connecting node:

$$h_1 m_{tot} = h_6 m_1 + h_9 m_2 + h_{11} m_3 \tag{5}$$

The actual enthalpy of the compressor's outlet can be determined by using its efficiency as shown:

$$\eta_c = \frac{h_{2isen} - h_1}{h_2 - h_1} \tag{6}$$

The rate of work of the compressor can be calculated as follows:

$$W_c = m_{tot}(h_2 - h_1) \tag{7}$$

Therefore, the coefficient of performance of the VRF system can be calculated as:

$$COP = \frac{Q_{evap1} + Q_{evap2} + Q_{evap3}}{W_c} \tag{8}$$

Since most air conditioning systems are oversized by design, the concept of part load performance has been developed recently defining a system that is not operating at

its full load capacity. The part load calculation can be a useful tool in analyzing the performance of a system operating at part load conditions.

The part load ratio (PLR) can be calculated as follows:

$$PLR = \frac{Pc_{cyc}}{Pc_{full}} \tag{9}$$

The part load factor (PLF) can be written as:

$$PLF = \frac{PLR}{aPLR + b} \tag{10}$$

where a and b are constants obtained from experimental work done by Bettanini et al. [11].

2.2 Results and Discussion

2.2.1 Base Model

The standard model of the VRF cycle runs with R-134a and the design compressor efficiency equal to 70%. All three evaporators have a cooling capacity of 12 kW each. Evaporator 1, evaporator 2, and evaporator 3 are set at a temperature equal to 4°C, 0°C, and -4°C. The condenser temperature is 40°C. There is no pressure drop in the evaporators and the condenser as shown in the P-h diagram in figure 2.2. There is no parasitic power input. The resultant coefficient of performance in this case was equal to 3.77 based on the entire set of the VRF cycle conditions.

2.2.2 Sensitivity Analysis

The coefficient of performance for the VRF system as a function of the condenser's temperature for R-134a with different evaporator's temperature is shown in Figure 2.3. The temperature of evaporator 1, evaporator 2, and evaporator 3 were set at 4°C, 0°C, and -4°C respectively. In figure 2.3, it can be noted that the coefficient of performance decreases as the outdoor temperature increases. The increment of the outdoor temperature, reduce the efficiency of the condenser and the amount of heat eliminate to the ambient. Therefore, the system has to do more work to maintain the same temperature by increasing the mass flow rate of the R-134a refrigerant. This effect causes the drop of the coefficient of performance for the VRF system.

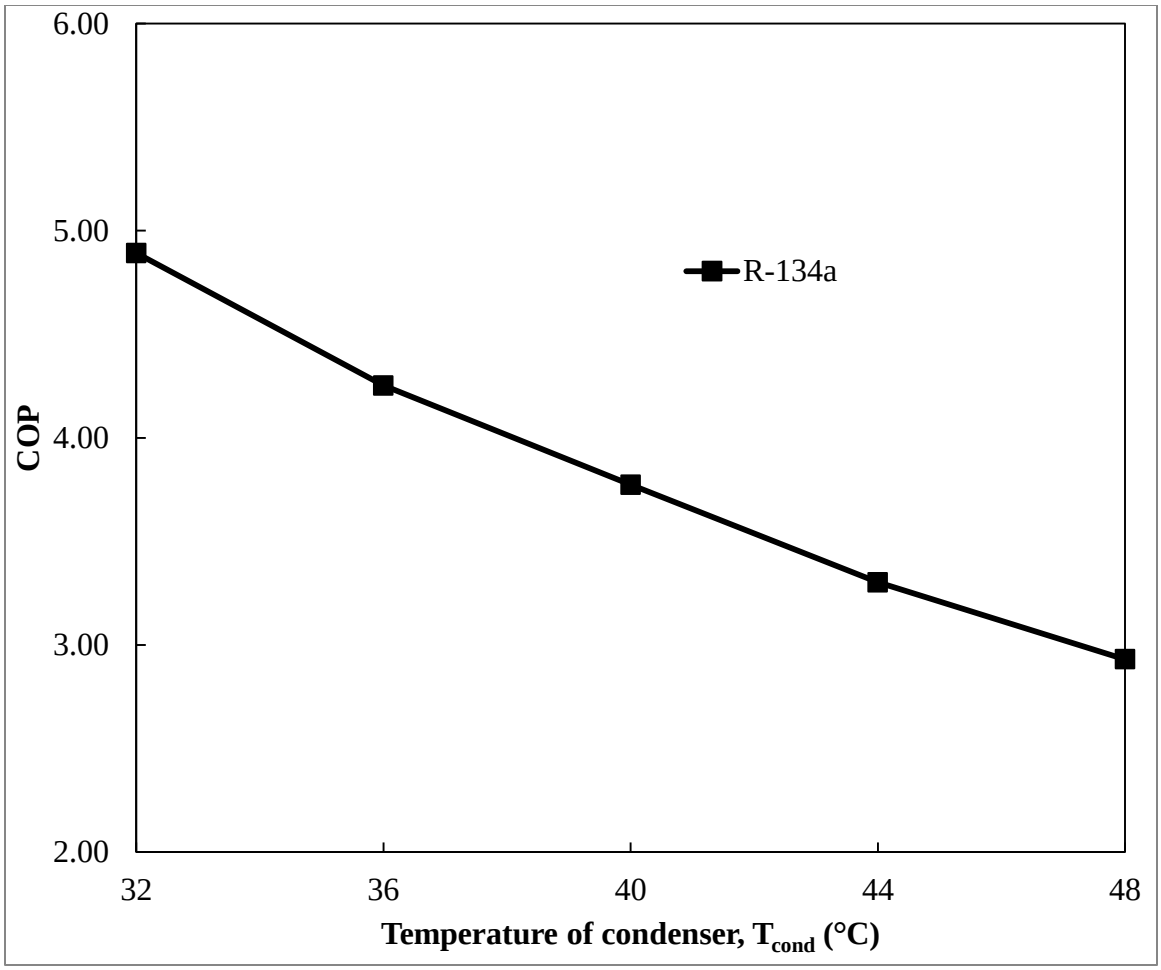

Figure 2.3: Effects of the temperature of the condenser on COP for R-134a (T_{evap1}= 4°C, T_{evap2}= 0°C, T_{evap3}= -4°C).

The coefficient of performance for the VRF system as a function of the condenser's temperature for R-134a with different evaporator's temperature is shown in Figure 2.4. The temperature of evaporator 1, evaporator 2, and evaporator 3 were set at 8°C, 0°C, and -8°C respectively. In figure 2.4, it can be noted that the coefficient of performance decreases as the outdoor temperature increases. The increment of the outdoor temperature, reduce the efficiency of the condenser and the amount of heat eliminate to the ambient. Therefore, the system has to do more work to maintain the same temperature by increasing the mass flow rate of the R-134a refrigerant. This effect causes the drop of the coefficient of performance for the VRF system. By comparing figure 2.3 to figure 2.4, one can notice a slight decrease of the COP when the range of evaporators' temperatures increases.

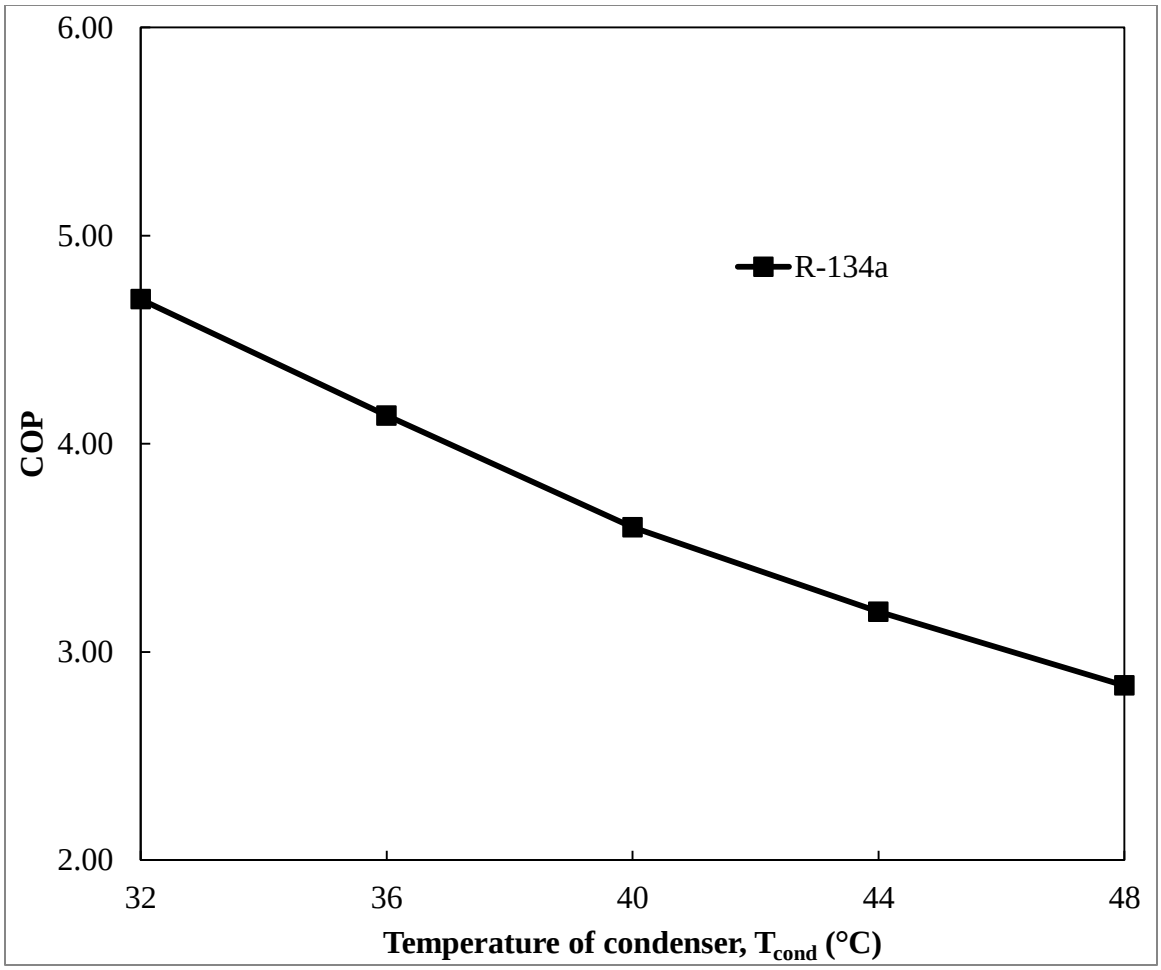

Figure 2.4: Effects of the temperature of the condenser on COP for R-134a (T_{evap1}= 8°C, T_{evap2}= 0°C, T_{evap3}= -8°C).

Figure 2.5 shows the effects of the cooling capacity of the evaporators on the rate of work of the compressor for R-134a. The range of the cooling capacities studies are 10-14 kW. All other conditions were kept at base condition. Figure 2.5 shows that as the cooling capacity of the system increases, the compressor rate of work increases. This is because the increase of the cooling capacity will increase the total mass flow rate of the system. Therefore, the compressor has to do more work to keep the other conditions constant.

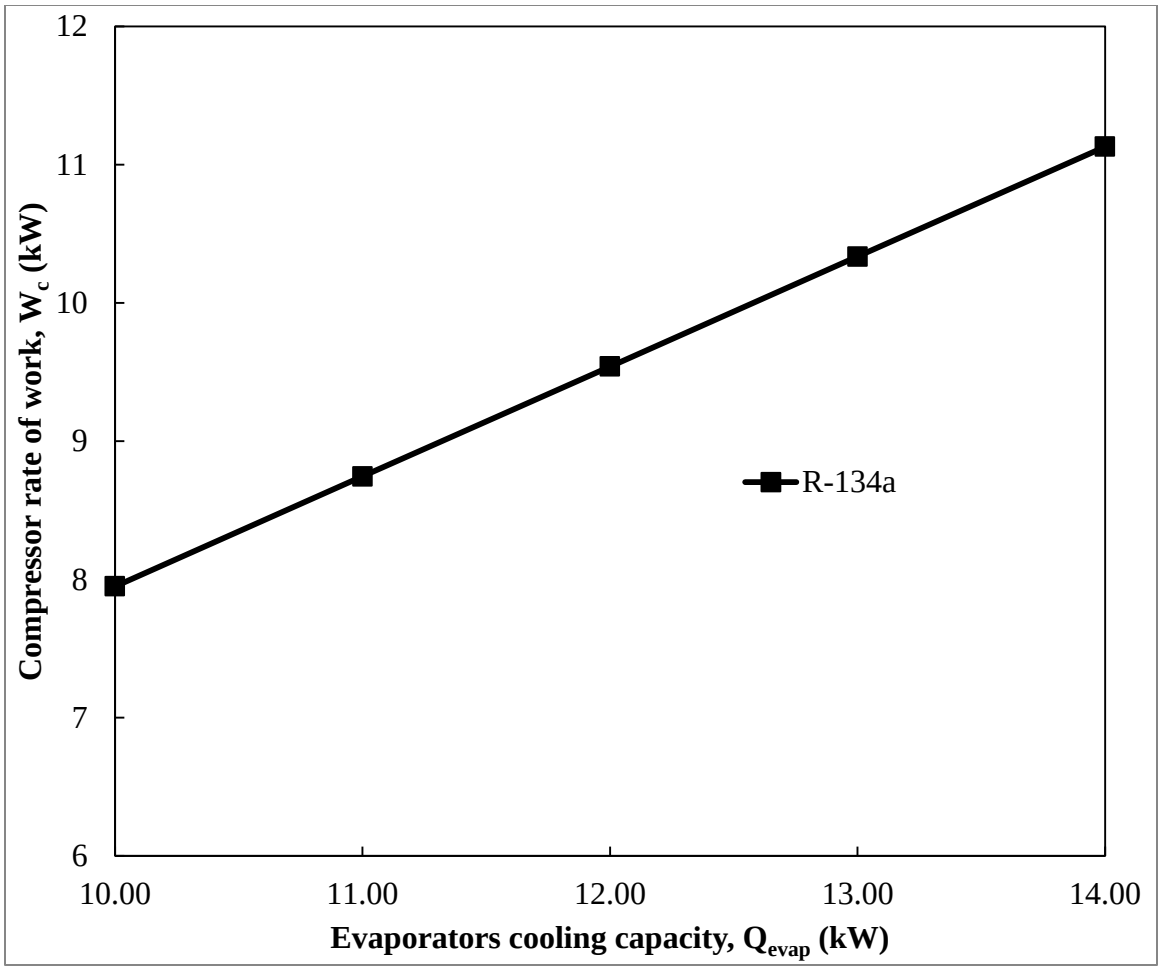

Figure 2.5: Effects of the cooling capacity of the evaporators on the compressor rate of work for R-143a (T_{evap1}= 4°C, T_{evap2}= 0°C, T_{evap3}= -4°C).

The effects of part load ratio (PLR) on part load factor (PLF) for refrigerant R-134a is shown in figure 2.6. All values of the system were taken at base condition. The first run was taken with 100% cooling load for each evaporator. At that time the VRF cycle was set to run at full load, the result was as expected with a PLF of 100% by using equation (10) and by calculating the PLR from equation (9). Subsequently, all of the evaporators were set at 75%, 50%, and 25% of the cooling load for the following additional runs. As expected the PLF results decreased with the reduction of the cooling load for the VRF system as shown in figure 2.6.

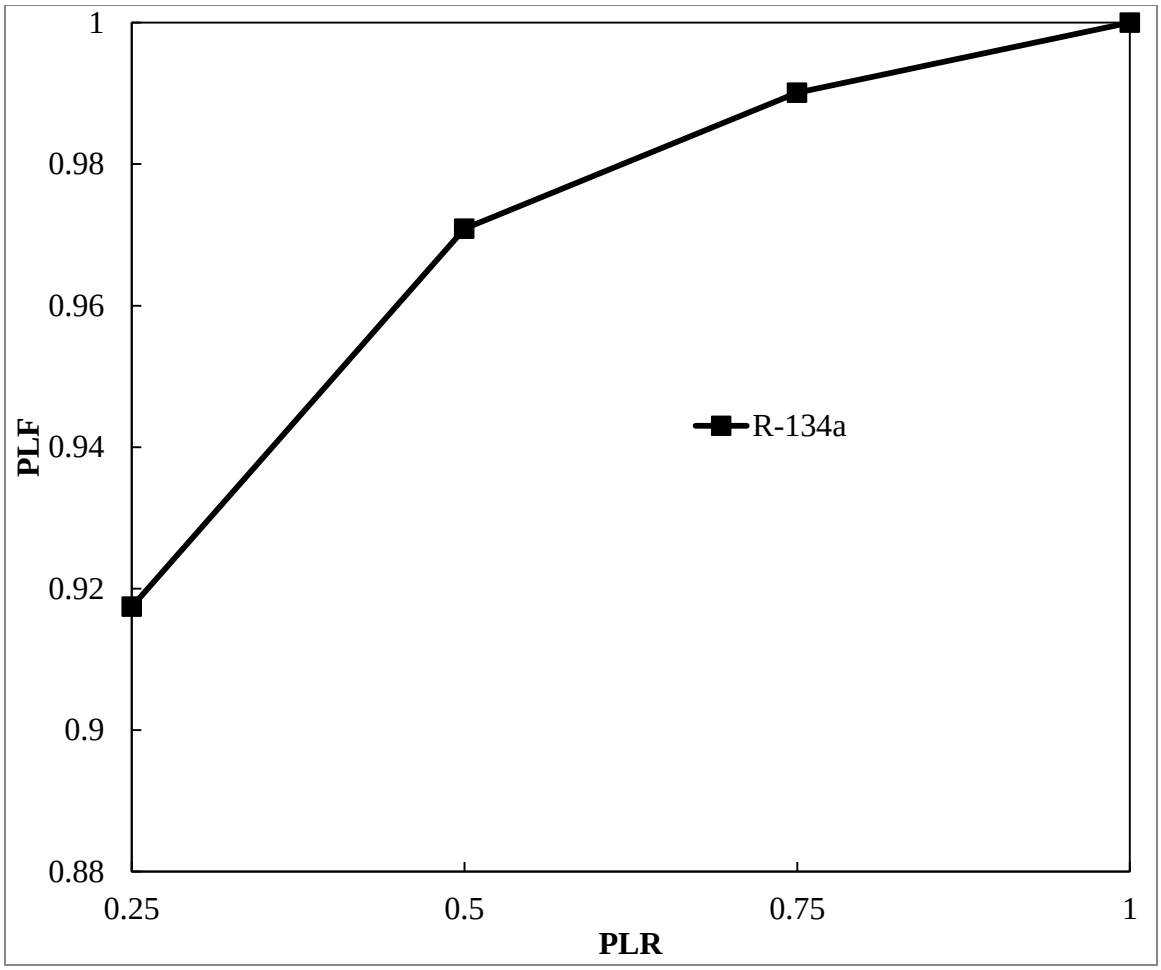

Figure 2.6: PLF versus PLR for R-134a (T_{evap1}= 4°C, T_{evap2}= 0°C, T_{evap3}= -4°C).

Figure 2.7 shows the effects of the temperature of the condenser on coefficient of performance for R-134a and R-22. The temperature of evaporator 1, evaporator 2, and evaporator 3 were set at 4°C, 0°C, and -4°C respectively. The coefficient of performance for R-134a was higher than R-22. This effect shows the ability of the R-134a refrigerant to reject more heat at the same condensing temperature when used for multiple evaporators' temperatures. Therefore, the system has to do less work to maintain the same temperature by using the R-134a refrigerant under the same VRF cycle conditions. The increment of the outdoor temperature, decrease the efficiency of the condenser and the coefficient of performance of the VRF system in general.

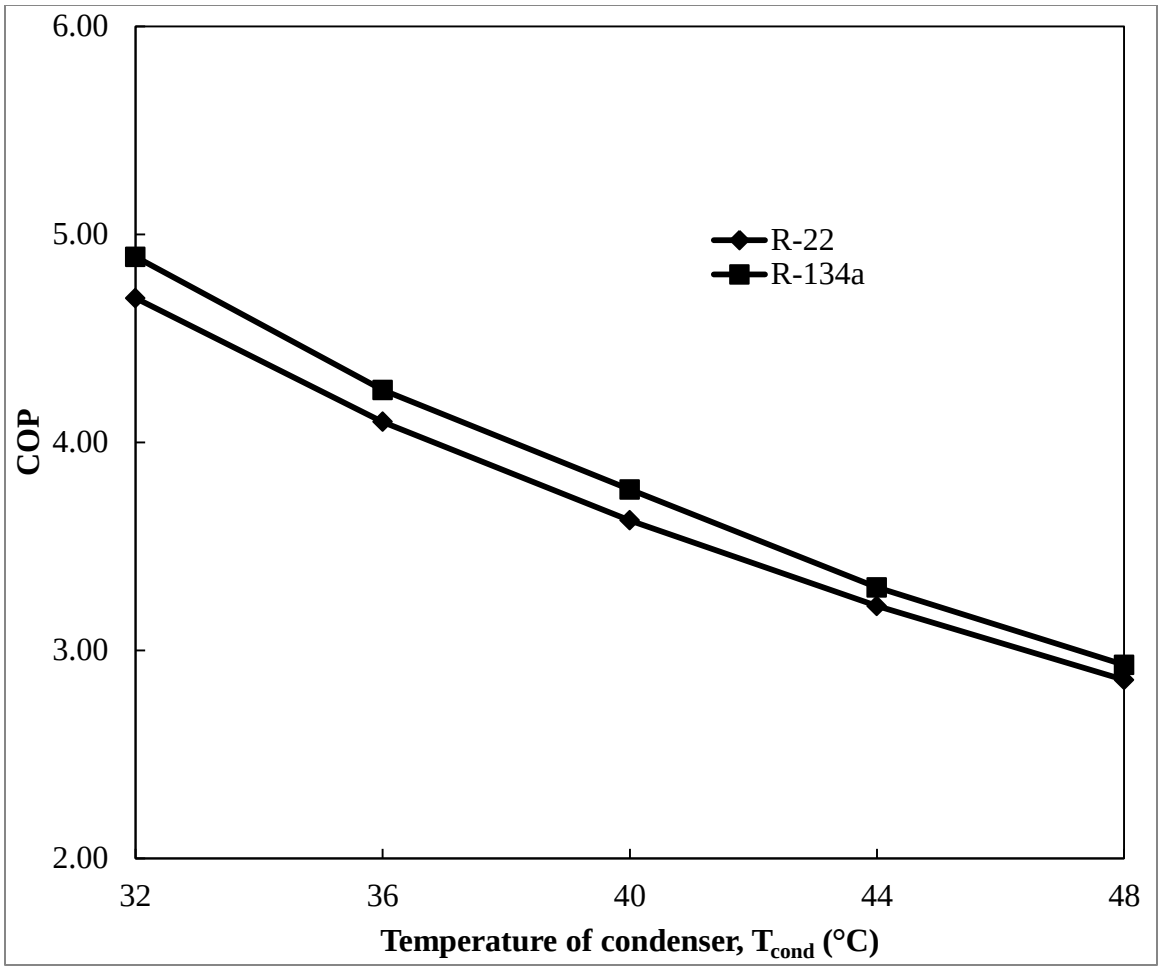

Figure 2.7: Effects of the temperature of the condenser on COP for R-22 and R-134a (T_{evap1}= 4°C, T_{evap2}= 0°C, T_{evap3}= -4°C).

Figure 2.8 shows the effects of the temperature of the condenser on coefficient of performance for R-134a and R-22. The temperature of evaporator 1, evaporator 2, and evaporator 3 were set at 8°C, 0°C, and -8°C respectively. The coefficient of performance for R-134a was higher than R-22. This effect shows the ability of the R-134a refrigerant to reject more heat at the same condensing temperature when used for multiple evaporators' temperatures.

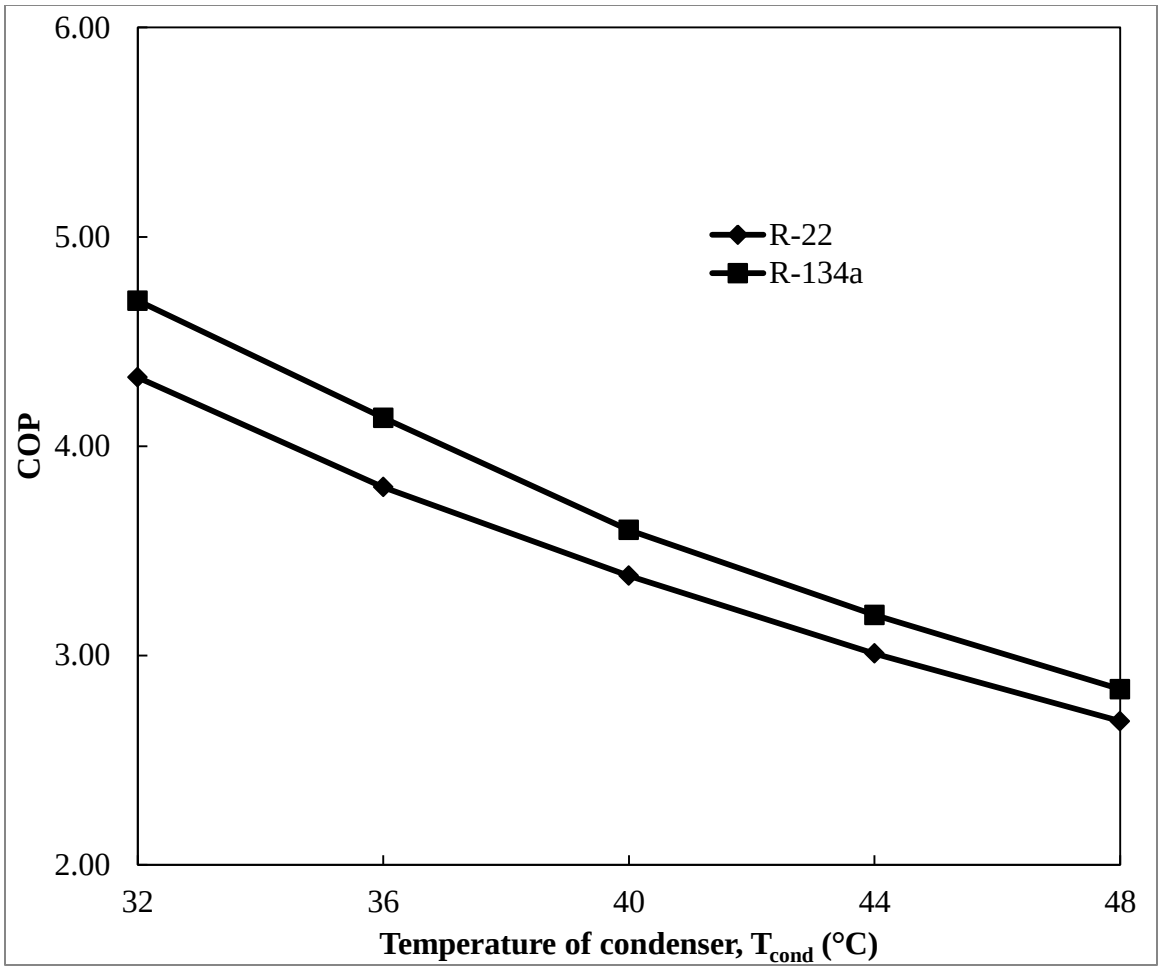

Figure 2.8: Effects of the temperature of the condenser on COP for R-22 and R-134a (T_{evap1}= 8°C, T_{evap2}= 0°C, T_{evap3}= -8°C).

Figure 2.9 shows the effects of the cooling capacity of the evaporators on the rate of work of the compressor for R-22 and R-134a. The range of the cooling capacities studies are 10-14 kW. All other conditions were kept at base condition. Figure 2.9 shows that as the cooling capacity of the system increases, the compressor rate of work increases. This is because the increase of the cooling capacity will increase the total mass flow rate of the system. Therefore, the compressor has to do more work in order to maintain the other conditions constant. Figure 2.9 also shows that the VRF system with R-134a uses less compressor power than a VRF system with R-22.

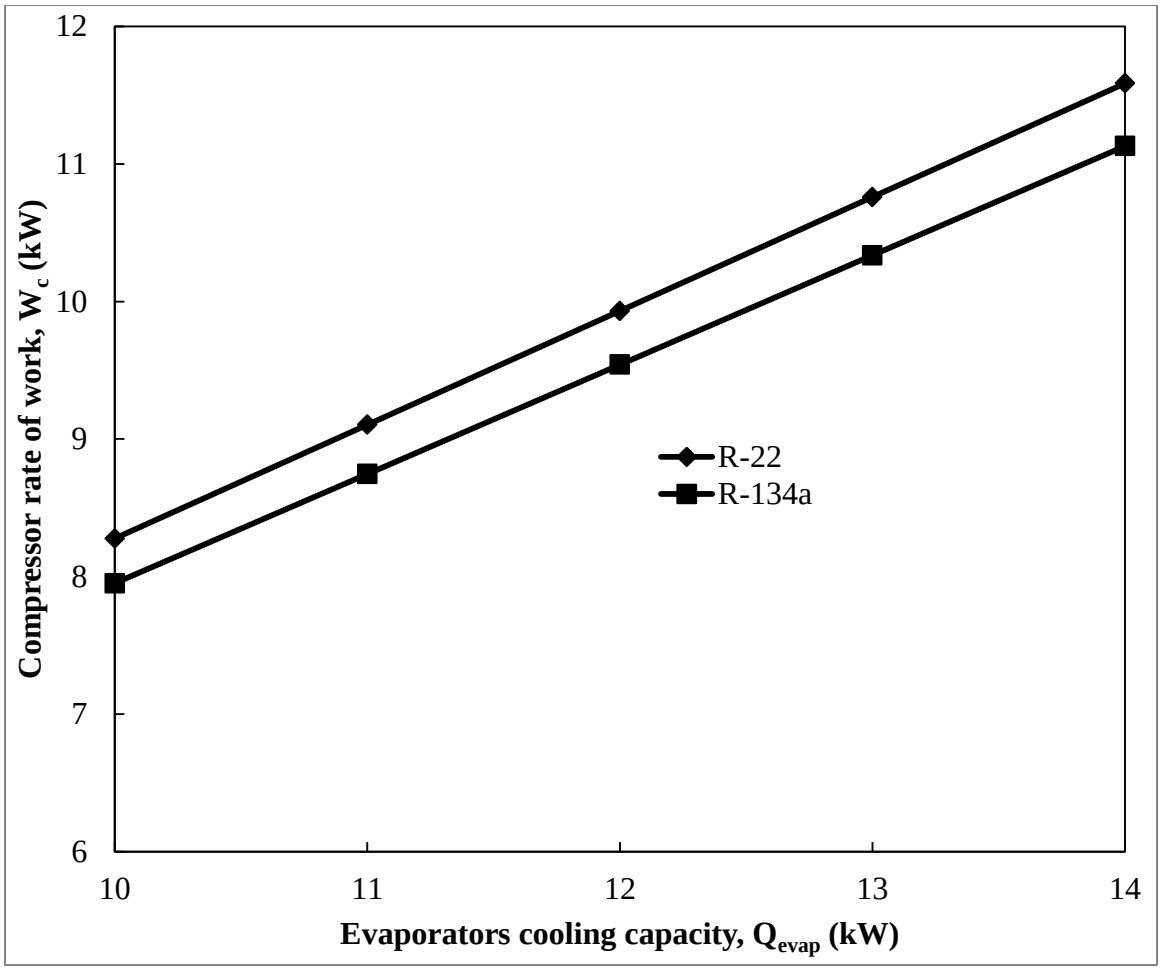

Figure 2.9: Effects of the cooling capacity of the evaporators on the compressor rate of work for R-22 and R-143a (T_{evap1}= 4°C, T_{evap2}= 0°C, T_{evap3}= -4°C).

Figure 2.10 shows the effects of PLF on PLR for refrigerants R-134a and R-22. All three of the evaporators were set at the base condition as well as the condensing temperature for all runs. The first run was taken with 100% cooling load for each evaporator. At that time the VRF cycle was set to run at full load and the result was as expected with a PLF of 100% by using equation (10) and by calculating the PLR from equation (9). Subsequently, all of the evaporators were set at 75%, 50%, and 25% of the cooling load for the following additional runs. The PLF results are almost identical for both refrigerants and decrease with the reduction of the cooling load of the VRF system as shown in figure 2.10.

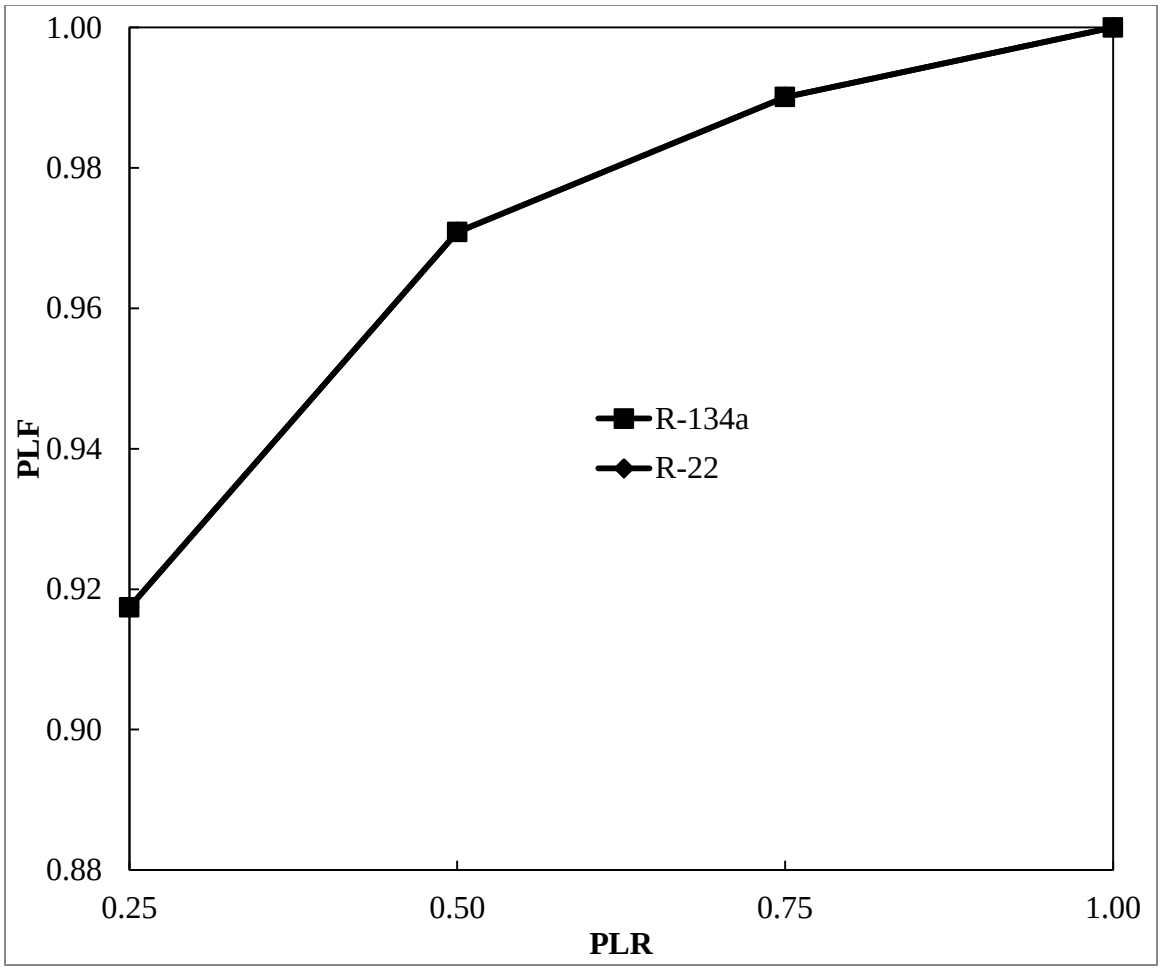

Figure 2.10: PLF versus PLR for R-22 and R-134a (T_{evap1}= 4°C, T_{evap2}= 0°C, T_{evap3}= -4°C).

The coefficient of performance as a function of the condenser's temperature of R-134a refrigerant for one and three evaporators is shown in figure 2.11. The 3 evaporators' cycle were kept at the base conditions, while the 1 evaporator cycle was set with a cooling capacity of 36 kW and evaporator temperature of 0°C. The following figure shows that the VRF cycle has lower coefficient of performance compared to vapor compression cycle. This is due to the different evaporators' temperatures which require different mass flow rates of the refrigerant; therefore, it affects the overall coefficient of performance.

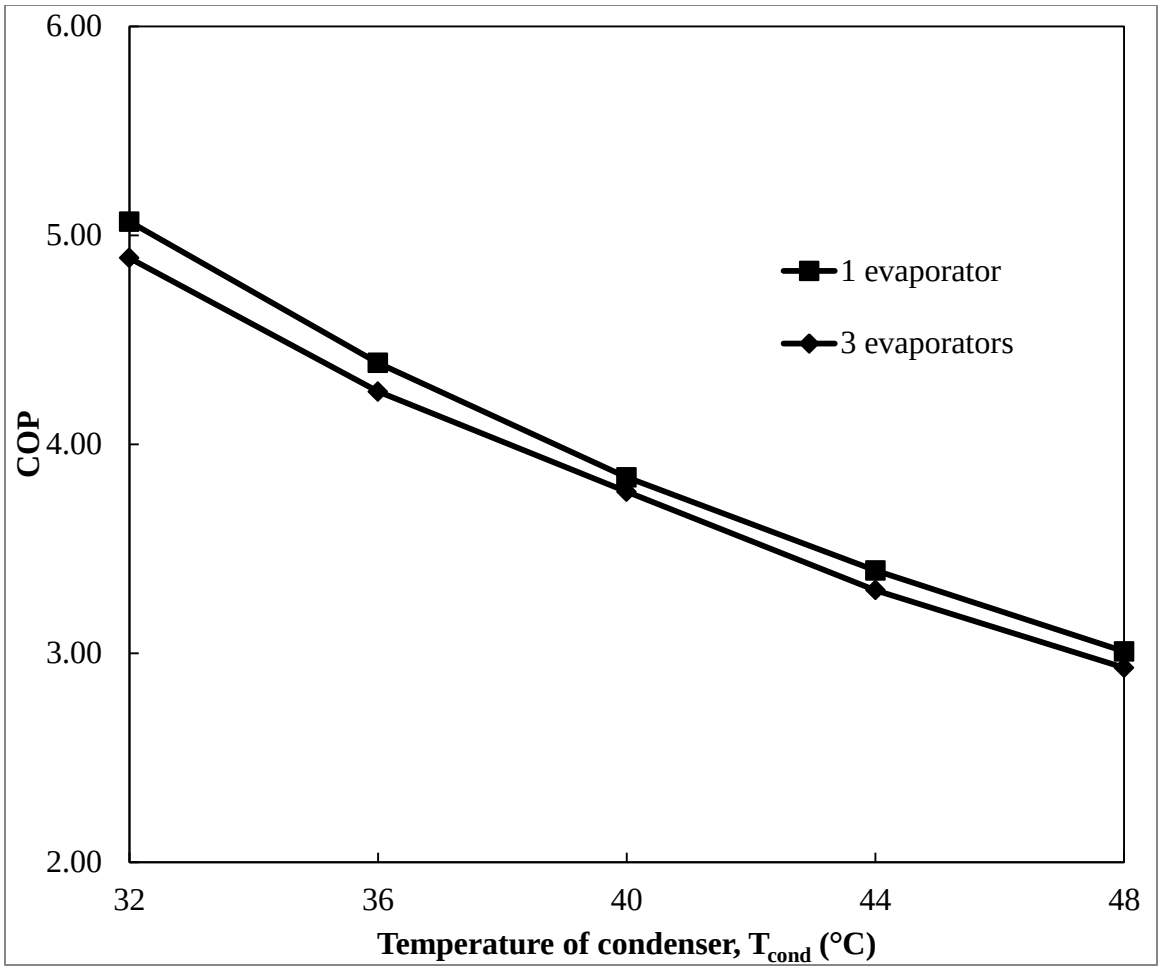

Figure 2.11: Effects of the temperature of the condenser on COP for one and multiple evaporators' cycle using R-134a.

Table 2.1 shows a comparison between the coefficients of performance obtained from Hitachi [29] and Toshiba [30] catalogs to the present coefficient of performance results for the VRF system. The Hitachi catalog has a VRF air conditioning system with a value of COP equal to 4.85, while the Toshiba catalog has a VRF air conditioning system with a value of COP equal to 4.61. The R-410a refrigerant was used in both catalogs. In our model the coefficient of performance, was determined by using the R-410a refrigerant as part of the cycle running under the same operating conditions for both catalogs. The simulated VRF air conditioning system had a COP value equal to 5.08. Present numerical COP results correlate with an average margin of 4.5%, and 9.2% with the Hitachi and Toshiba catalog respectively.

Table 2.1: Comparison between simulated COP and experimental COP for R-410a.

	Present Result	Experimental	
COP	5.08	4.85[29]	4.61[30]

Our simulated model ignored any pressure drop in the condenser and the evaporators units due to friction and heat transfer. All these conditions will affect the COP of the simulated VRF system if they have been taken into account. The difference between the two experimental values might come from the differences in pipe lengths which affects the friction and the heat transfer. In addition, the differences between the compressor's performance for each manufacturer might have been influenced the results.

Chapter 3: Exergy Analysis of a Typical Air Conditioning System

3.1 Mathematical Model

Figure 3.1 shows a schematic diagram of the air conditioning system that supply air to a specific temperature controlled room. The air passing through the dehumidifier or condensing unit is a mixture of the outside fresh air and a portion of the bypassed air coming from the air conditioned room. A fraction of the return air from the room is exhausted to the environment to maintain the mass balance of the system. The amount of air to be exhausted or bypassed depends on the nature of the conditioned space. In highly contaminated environments such as hospital rooms or welding shops, the system is designed with no bypass, whereas in a typical residential room a large amount of bypass air can be used to save energy.

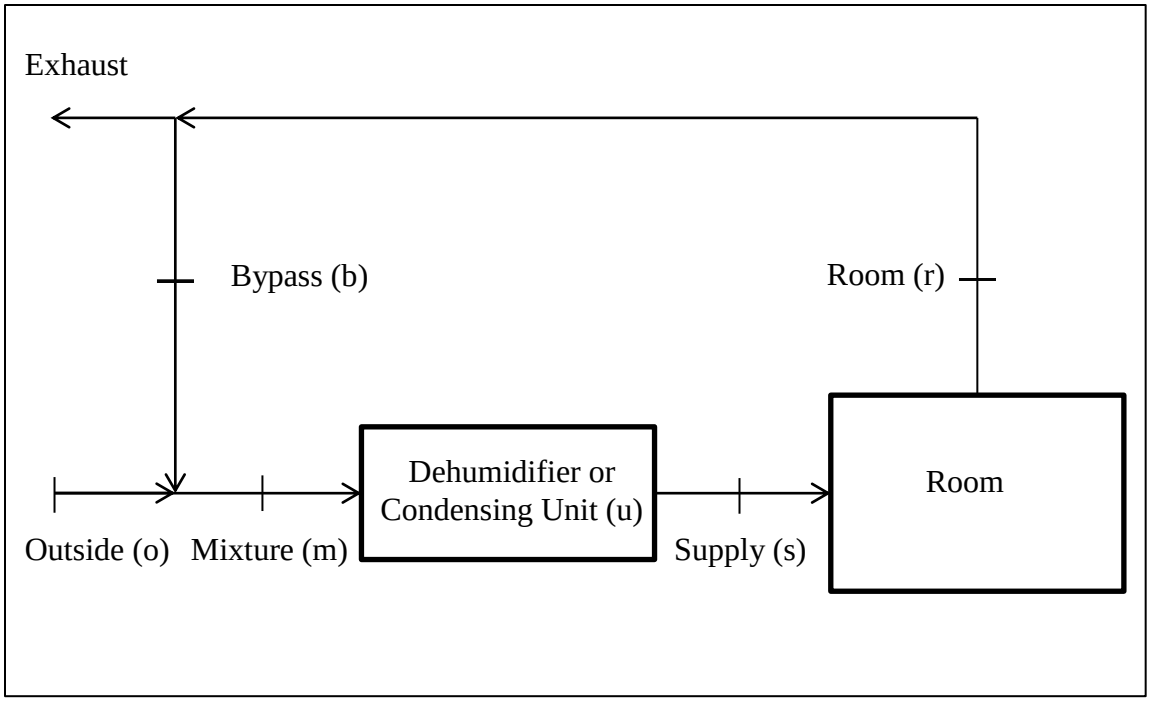

Figure 3.1: Schematic diagram of the air conditioning system.

The base model of the A/C system was taken at outside air temperature (T_o= 35^{o}C) and relative humidity (RH_o = 70%), sensible heat (Q_{sen} = 12.30 kW), latent heat (Q_{lat} = 3.51 kW), room air temperature (T_r= 20^{o}C), and relative humidity (RH_r= 40%), outside air flow rate (q_o = 0.38 m^3/s), and bypass air flow rate (q_b = 0.61 m^3/s). The range of parameters covered in the analysis included outside air temperature (T_o= 25-60^{o}C) and relative humidity (RH_o = 50-85%), sensible heat (Q_{sen} = 11.50-13.25 kW), latent heat (Q_{lat} = 3.00-4.75 kW), room air temperature (T_r= 18-25^{o}C), and relative humidity (RH_r= 30-44%), and outside-mixture air flow rate ratio (q_o/q_m= 0.21-0.71).

The mathematical formulation of an air conditioning system takes into account the mass balance of dry air and water, the energy balance by applying the first law of thermodynamics, and the entropy or exergy balance by using the second law of thermodynamics. The air and water properties were obtained from the ASHRAE Handbook of Fundamentals [31]. The equations describing the conservation of mass, energy, entropy and exergy balance for different processes can be written as:

Adiabatic Mixing of Air Streams

Dry air mass balance:

$$m_{ao} + m_{ab} = m_{am} \tag{11}$$

Water mass balance:

$$m_{wo} + m_{wb} = m_{wm} \tag{12}$$

Energy balance:

$$m_{ao}h_o + m_{ab}h_b = m_{am}h_m \tag{13}$$

Entropy balance:

$$m_{ao}s_o + m_{ab}s_b - m_{am}s_m + S_{gen} = 0 \tag{14}$$

Exergy balance:

$$m_{ao}\psi_o + m_{ab}\psi_b - m_{am}\psi_m - Ex_{dead} = 0 \tag{15}$$

$$Ex_{d,AM} = T_{dead}S_{gen} = T_{dead}(m_{am}s_m - m_{ao}s_o - m_{ab}s_b) \tag{16}$$

Dehumidifier or Condensing Unit

Dry air mass balance:

$$m_{am} = m_{as} \tag{17}$$

Water mass balance:

$$m_{wm} - m_w = m_{ws} \tag{18}$$

Energy balance:

$$m_{am}h_m = m_{as}h_s + Q_{out} + m_w h_w \tag{19}$$

Entropy balance:

$$m_{am}s_m - m_w s_w - \frac{Q_{out}}{T} - m_{as}s_s + S_{gen} = 0 \tag{20}$$

Exergy balance:

$$m_{am}\psi_m - Q_{out}(1 - \frac{T_{dead}}{T}) - m_{as}\psi_s - m_w\psi_w - Ex_d = 0 \tag{21}$$

$$Ex_{d,u} = T_{dead}S_{gen} = T_{dead}(m_{as}s_s + m_w s_w + \frac{Q_{out}}{T} - m_m s_m) \tag{22}$$

Control Room

Dry air mass balance:

$$m_{as} = m_{ar} \tag{23}$$

Water mass balance:

$$m_{ws} + m_w = m_{wr} \tag{24}$$

Energy balance:

$$m_{as}h_s + Q_{in} + m_w h_w = m_{ar}h_r \tag{25}$$

Entropy balance:

$$m_{as}s_s + m_w s_w + \frac{Q_{in}}{T} - m_{ar}s_r + S_{gen} = 0 \tag{26}$$

Exergy balance:

$$m_{as}\psi_s + Q_{in}(1 - \frac{T_{dead}}{T}) - m_{ar}\psi_r + m_w\psi_w - Ex_d = 0 \tag{27}$$

$$Ex_{d,r} = T_{dead}S_{gen} = T_{dead}(m_{ar}s_r - m_w s_w - \frac{Q_{in}}{T} - m_s s_s) \tag{28}$$

Therefore, total exergy destruction of the system can be written as:

$$Ex_{d,sys} = Ex_{d,AM} + Ex_{d,u} + Ex_{d,r} \tag{29}$$

The exergy efficiency of the system can be expressed as:

$$\eta_{ex,sys} = \frac{Ex_{out}}{Ex_{in}} = 1 - \frac{Ex_{d,sys}}{Ex_{in}} \tag{30}$$

The sensible heat ratio (SHR) of the air conditioning system can be written as:

$$SHR = \frac{Q_{sen}}{Q_{sen} + Q_{lat}} \tag{31}$$

3.2 Results and Discussion

The results of the exergy analysis are presented in terms of the outside conditions, room conditions, including room sensible and latent heat loads, and dead state effects on the exergy efficiency and exergy destruction of the A/C system. The dead state temperature selection for case 1 is equal to the outside fresh air temperature. On the other hand, the dead state temperature selection for case 2 is equal to 25°C.

Figure 3.2 shows the effects of the room latent heat load (Q_{lat}) on exergy efficiency and exergy destruction of the A/C system. All other room and outside conditions were set equal to the base model. The figure below shows that as room latent heat load increases, exergy destruction decreases and exergy efficiency increases. This is due to the fact that the A/C system has to decrease the air relative humidity of the supply in order to maintain the room conditions when the latent heat load increases. It's interesting to observe that the change in supply air relative humidity has a smaller effect on exergy destruction. By comparing case 1 to case 2, one can say that higher dead state temperatures increase the exergy destruction and exergy efficiency of the A/C system.

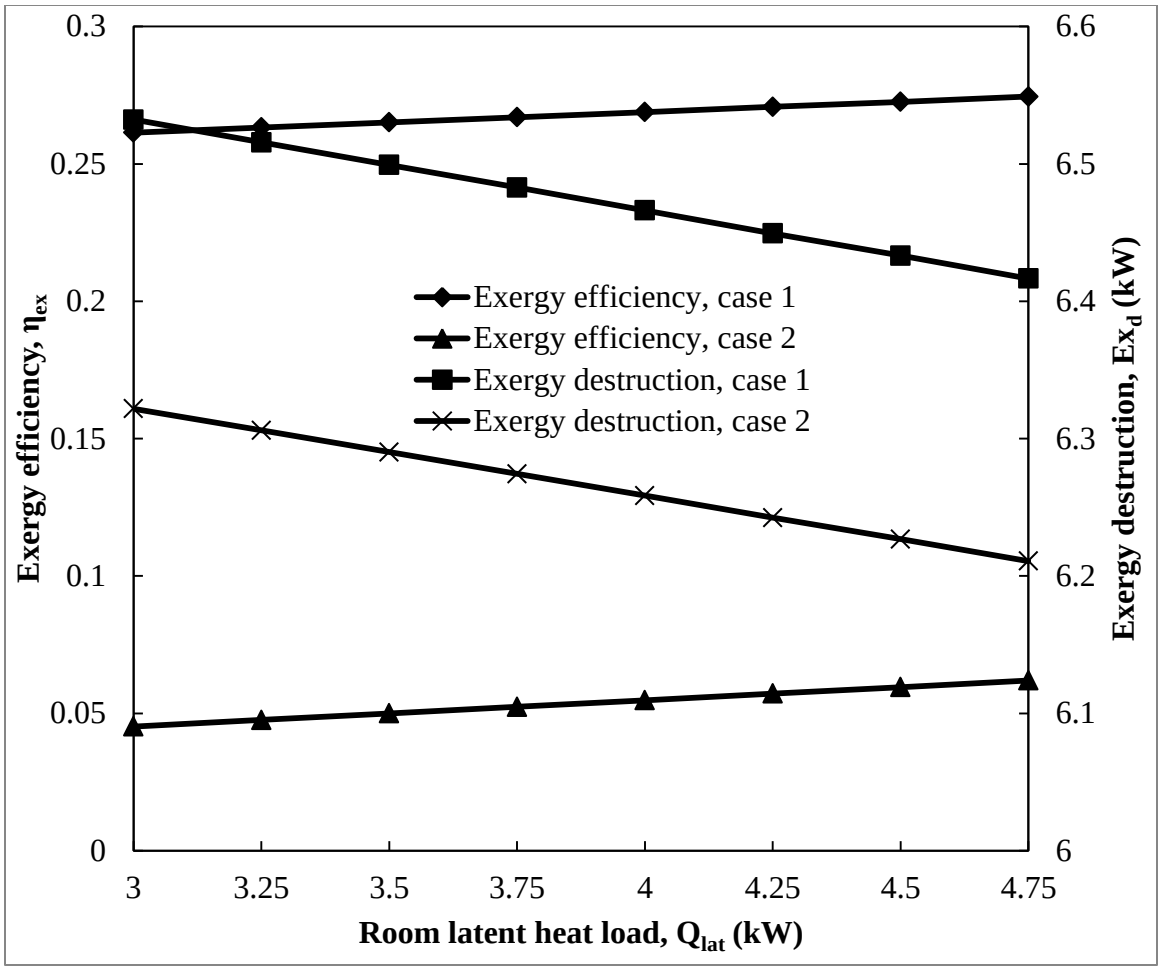

Figure 3.2: Effects of the room latent heat load (Q_{lat}) on exergy efficiency and exergy destruction of the A/C system.

Figure 3.3 shows the effects of the room's sensible heat load (Q_{sen}) on the exergy efficiency and exergy destruction of the A/C system. All other room and outside conditions were set equal to base model. The following figure illustrates that as room sensible heat load increases, exergy destruction increases and exergy efficiency decreases. This is opposite to the trend seen in figure 3.2. The reason is that the system has to supply the room with lower air temperature in order to maintain the other room conditions when sensible heat load increases. Also it's interesting to note that the change of the supply air temperature has a greater effect on exergy destruction than the change in supply air relative humidity. On the other hand, the effect of the dead state temperature is the same as discussed in figure 3.2.

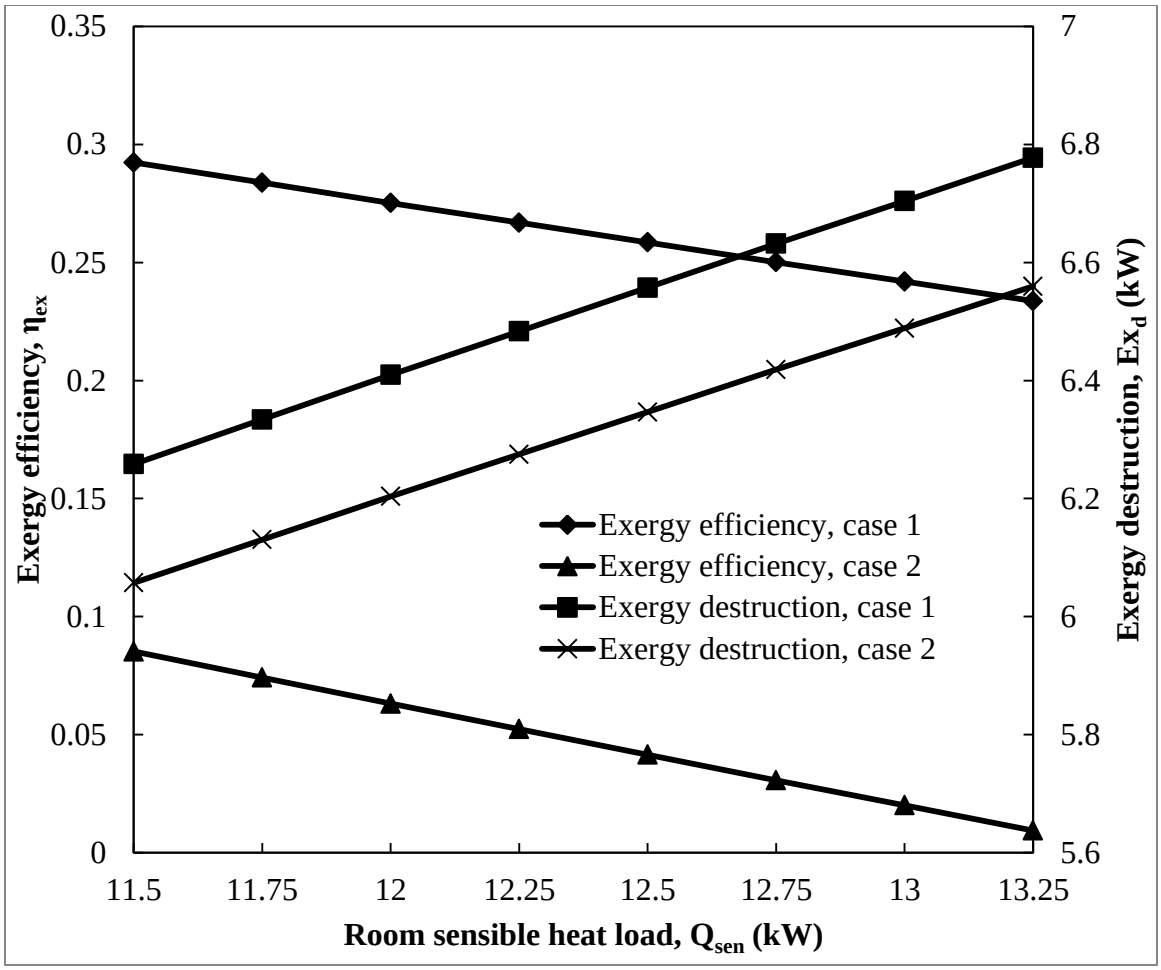

Figure 3.3: Effects of the room sensible heat load (Q_{sen}) on exergy efficiency and exergy destruction of the A/C system.

Figure 3.4 shows the effects of the room sensible and latent heat loads (Q_{lat}, Q_{sen}) on the exergy efficiency and exergy destruction of the A/C system for case 1. The calculation was conducted for the dead state temperature of 35°C which is the same as the outside air temperature. The outside and room air conditions were kept as our base model. Figure 3.4 plots the results as a function of sensible heat ratio (SHR) which is frequently used for designing or sizing an air conditioning system. The changes of the room sensible or latent heat load directly influence the SHR. In this figure, the SHR was calculated by independently varying the sensible heat load and latent heat load while keeping the other constants at the base value and plotted values of exergy destruction and exergy efficiency corresponding to both of these variations. It can be noticed that as room SHR increases, the exergy destruction increases and the exergy efficiency of the system decreases. This is due to the fact that as the exergy destruction increases and the exergy input remains the same since our outside conditions were constant; therefore, the exergy efficiency of the A/C system decreases. This relationship can be seen in equation (30). It is also interesting to note that sensible heat load has stronger influence on the variation of exergy destruction or exergy efficiency than when compared to latent heat load over the same range of the variation of SHR. This is because the smaller value required for latent heat load to change the SHR with the same increment when varying sensible heat load. Therefore, it may be more appropriate to consider Q_{sen} and Q_{lat} independently instead of SHR when designing an air conditioning system for improved exergy efficiency.

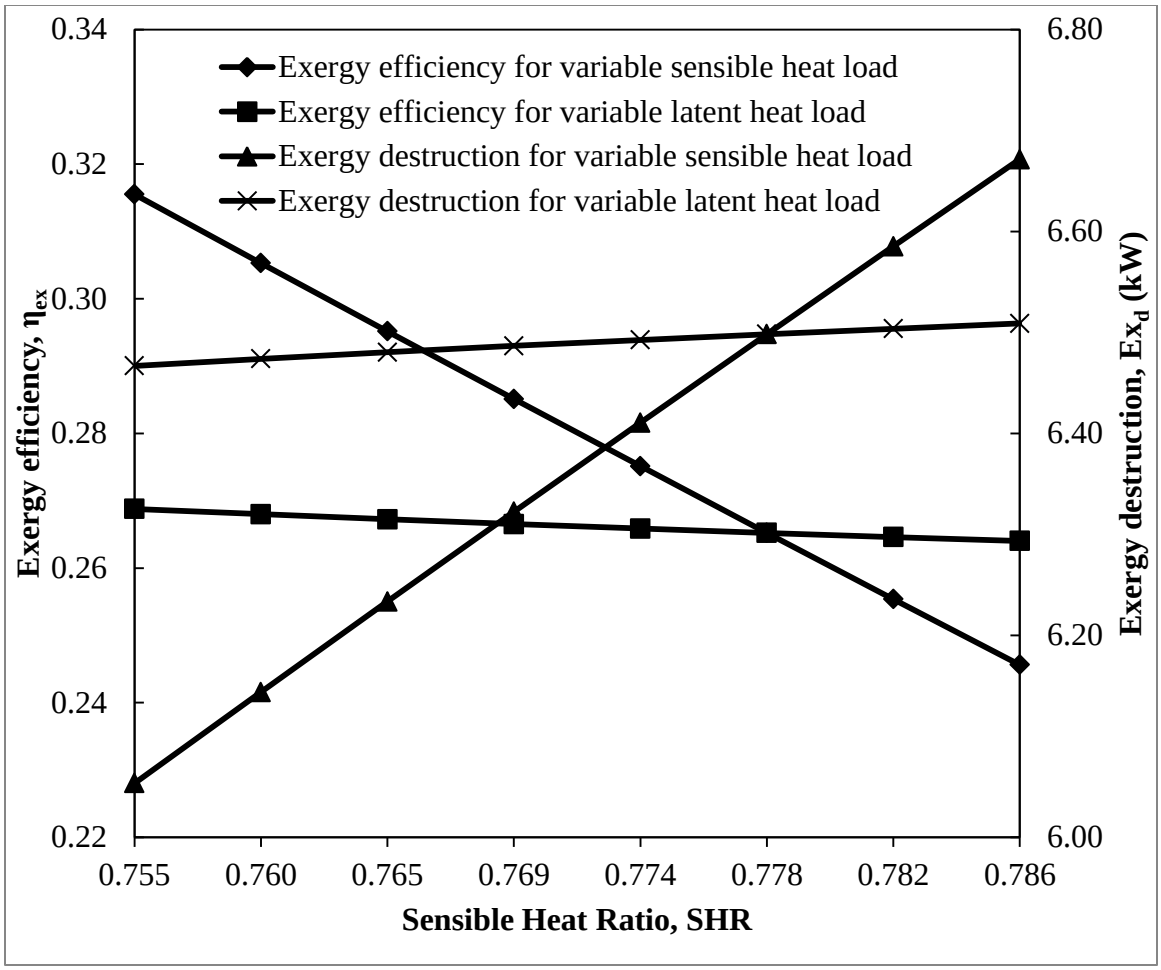

Figure 3.4: Effects of the room sensible and latent heat loads (Q_{sen}, Q_{lat}) on exergy efficiency and exergy destruction of the A/C system as a function of the SHR of the room ($T_{dead}= T_o$).

Figure 3.5 shows the effects of the room sensible and latent heat loads (Q_{lat}, Q_{sen}) on the exergy efficiency and exergy destruction of the A/C system for case 2. The calculation was conducted for the dead state temperature of 25°C. The outside and room air conditions were kept the same as our base model. The changes of the room latent heat load directly influence the SHR. This effect shows that the increment of the room SHR increases the exergy destruction and decreases the exergy efficiency of the system. This behavior occurs since the exergy input remains the same due to constant outside conditions; therefore, the exergy efficiency of the system decreases. Through comparison of figures 3.4 and 3.5, it can be observed that as the dead state temperature decreases, the exergy destruction and exergy efficiency of the A/C system decreases. The reason that the exergy efficiency decreases is due to the decrease of the exergy input at a greater rate than the exergy destruction of the system for different dead state temperatures.

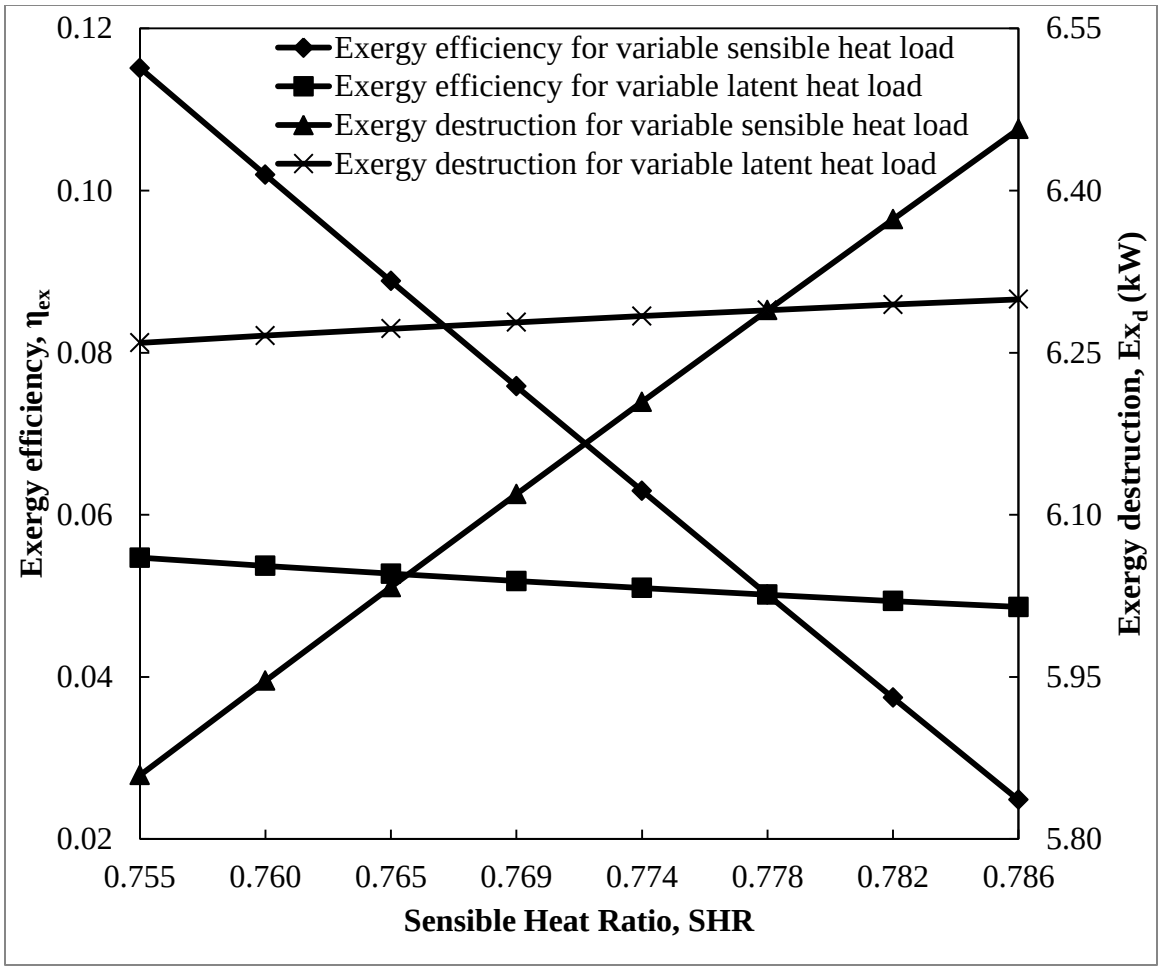

Figure 3.5: Effects of the room sensible and latent heat loads (Q_{sen}, Q_{lat}) on exergy efficiency and exergy destruction of the A/C system as a function of the SHR of the room (T_{dead}= 25^{o}C).

Figure 3.6 shows the effects of the outside air temperature (T_o) on exergy efficiency and exergy destruction. The dead state temperature was set equal to the outside air temperature for case 1 and equal to 25°C for case 2. The room air temperature, air relative humidity and outside air relative humidity were kept the same as our base model. Case 1 shows that as outside air temperature increases, the exergy destruction increases exponentially. On the other hand, the exergy efficiency of the A/C system shaped as a parabola opens downwards with a maximum value at 45°C. The reason for the trend observed in case 1 is due to the fact that the exergy input of the system increases in a constant rate while the exergy destruction of the system increases at higher rates after 40°C of outside air temperature. Case 2 shows that as outside air temperature increases, the exergy destruction increases exponentially. On the other hand, the exergy efficiency of the A/C system shapes as a parabola opens upwards with a minimum value at 40°C. This is due to the fact that the exergy input of the system increases at a higher rate than exergy destruction for higher outside air temperatures, therefore, it increases the exergy efficiency of the A/C system.

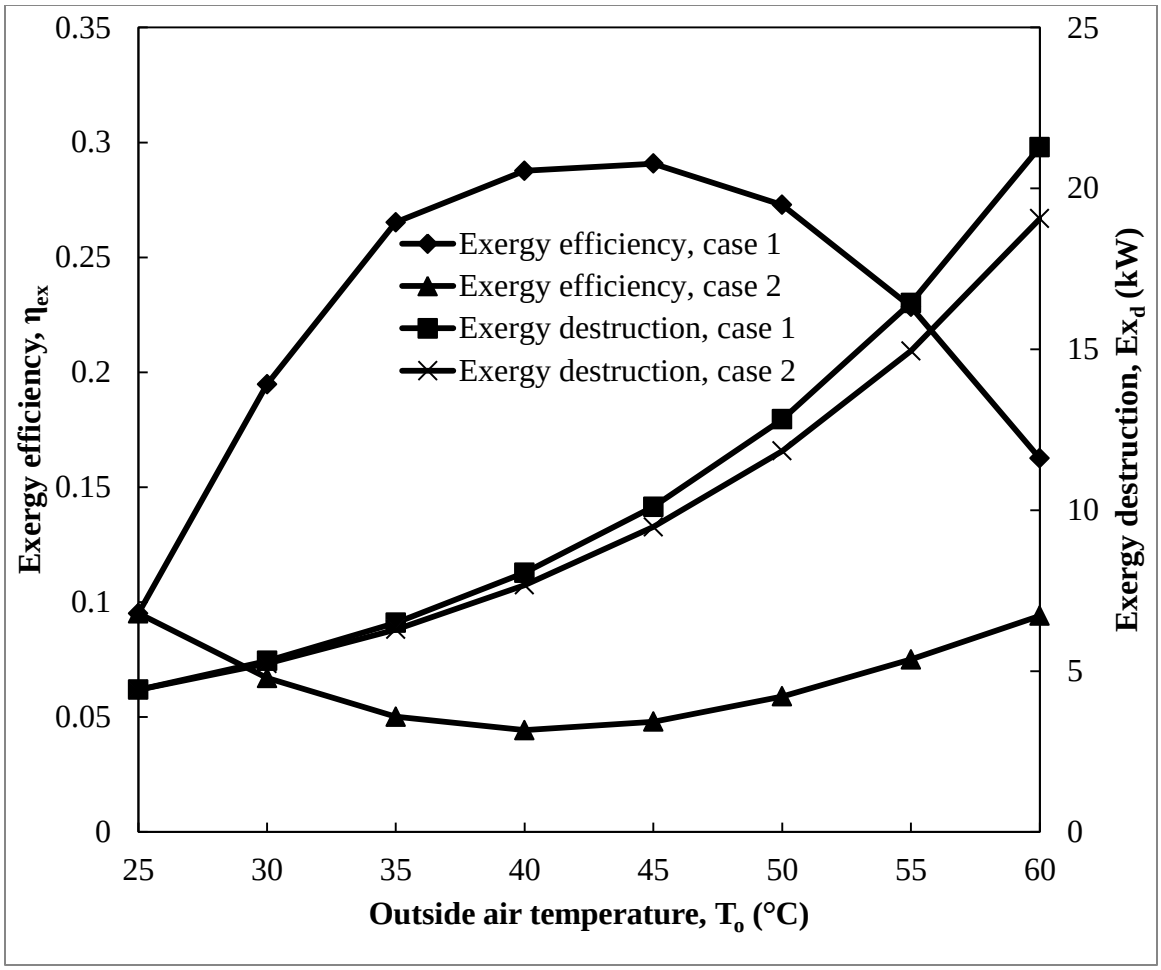

Figure 3.6: Effects of the outside air temperature (T_o) on exergy efficiency and exergy destruction of the A/C system.

The effects of the room air temperature (T_r) on exergy efficiency and exergy destruction are shown in figures 3.7 for both cases. The outside conditions and room relative humidity were kept as our base model. Figure 3.7 shows that as the room air temperature increases, the exergy destruction decreases until it reaches a minimum value at 23°C then it starts to increase. On the other hand, the exergy efficiency of the A/C system increases almost linearly. The reason behind the linear increasing in the exergy efficiency is the higher increasing rate in the exergy input when the exergy destruction starts to increase again. The analysis holds true for both cases and the effects of the dead state temperature follow the same trend discussed in previous figures.

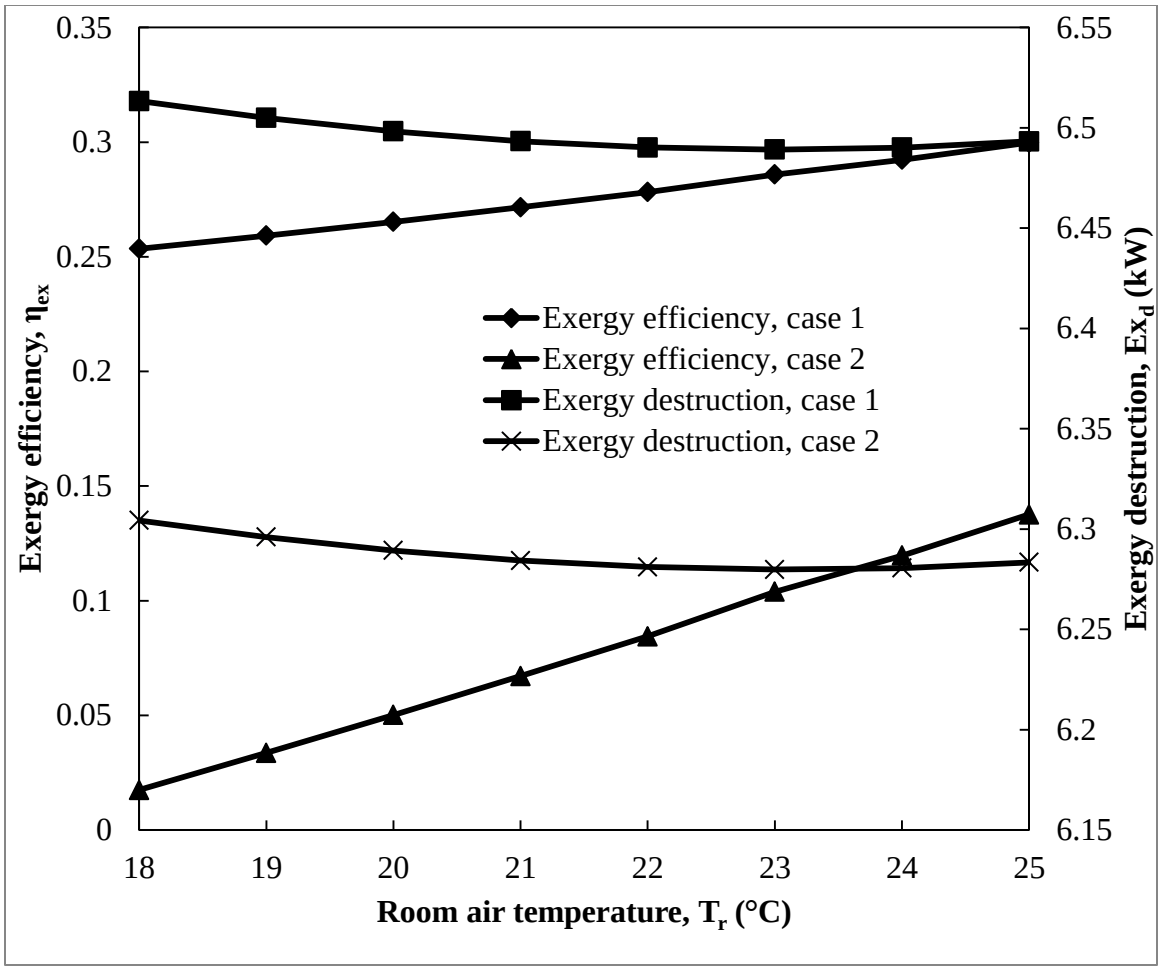

Figure 3.7: Effects of the room air temperature (T_r) on exergy efficiency and exergy destruction of the A/C system.

The effects of outside air relative humidity (RH_o) on exergy efficiency and exergy destruction of the A/C system are shown in figure 3.8. The outside temperature and room conditions were kept at the same conditions as our base model. Figure 3.8 shows that the increment of the outside air relative humidity increases the exergy destruction and decreases the exergy efficiency of the A/C system. This behavior occurs because the exergy input increases at a slower rate than the exergy destruction; therefore, the exergy efficiency of the system decreases. The effects of the dead state temperature follow the same trends discussed in previous figures.

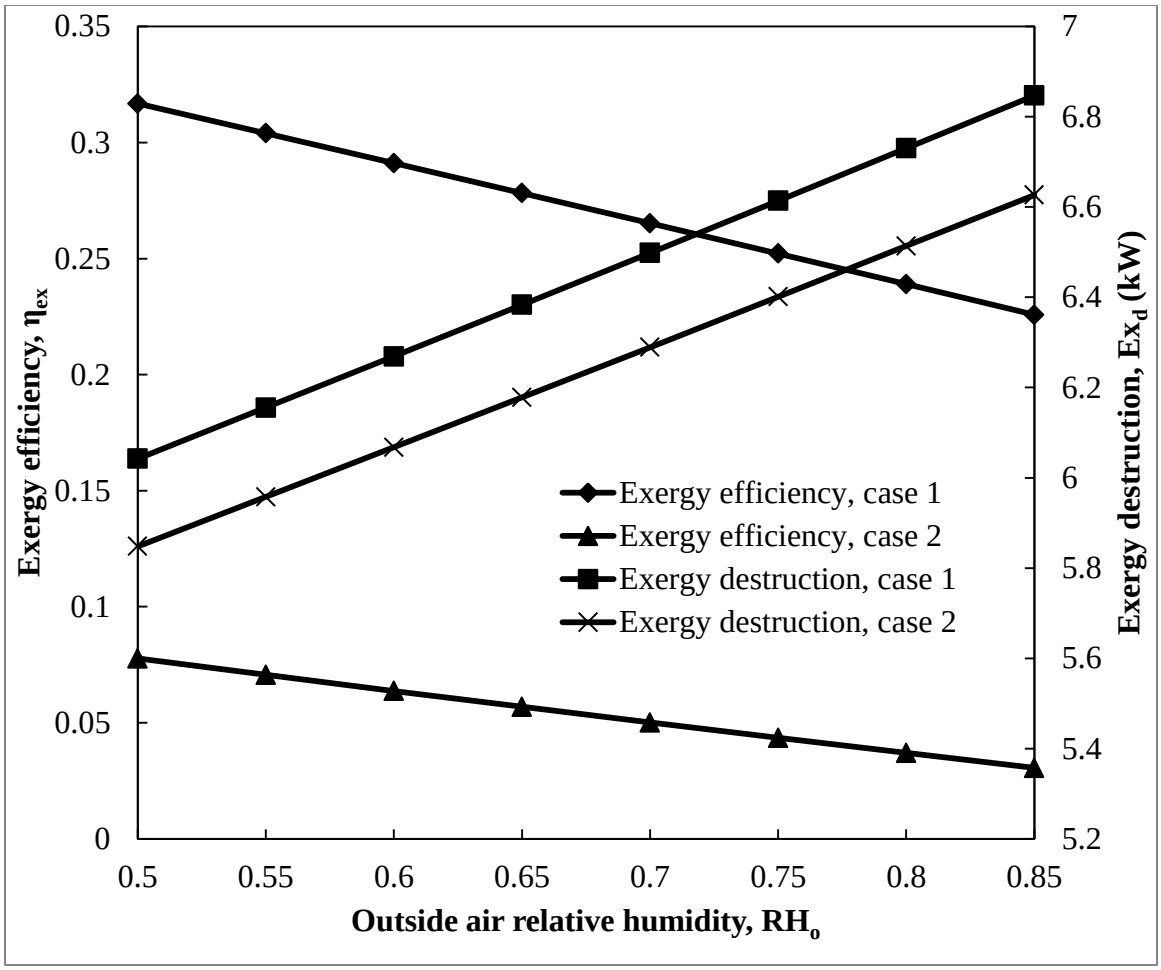

Figure 3.8: Effects of outside air relative humidity (RH_o) on exergy efficiency and exergy destruction of the A/C system.

The room relative humidity (RH_r) effects on the exergy efficiency and exergy destruction of the A/C system are illustrated in figure 3.9. The outside conditions and room air temperature were again kept as our base model. Figure 3.9 shows that the increment of the room relative humidity of the A/C system increases the exergy destruction and decreases its exergy efficiency. This effect is due to the smaller increment of the exergy input in comparison with the exergy destruction of the A/C system. Additionally, the increment of the dead state temperature increases the exergy destruction and exergy efficiency of the A/C system.

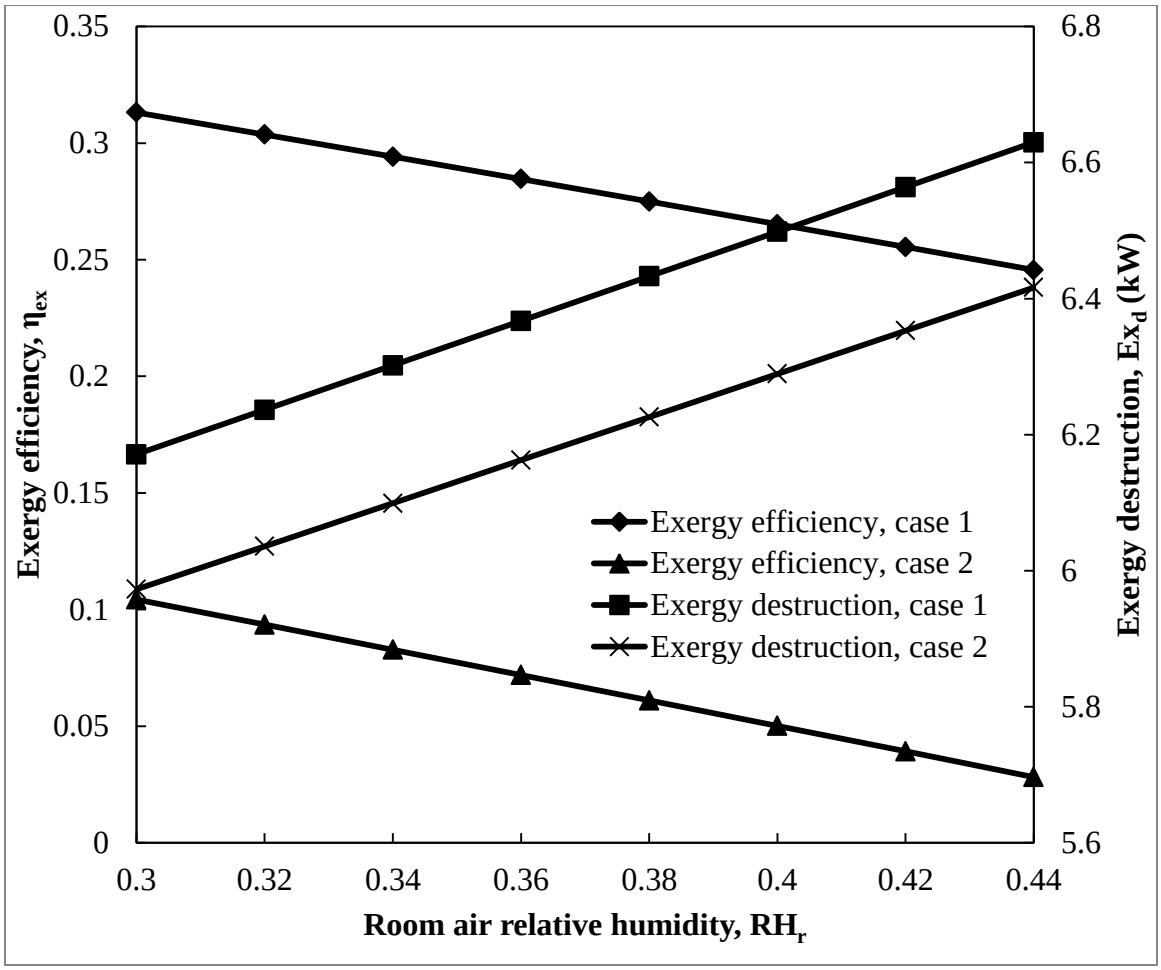

Figure 3.9: Effects of the room air relative humidity (RH_r) on exergy efficiency and exergy destruction of the A/C system.

Figure 3.10 shows the effects of outside to mixture air flow rate ratio (q_o/q_m) on exergy efficiency and exergy destruction. The dead state temperature was kept at 35^{o}C. The outside and room air conditions were kept the same as our base model. Figure 10 shows that by increasing the outside-mixture air flow rate ratio from 21% to 71% of the total air flow, the exergy destruction increases and the exergy efficiency decreases. This is due to the higher increasing rate of exergy destruction when compared to the exergy input of the A/C system.

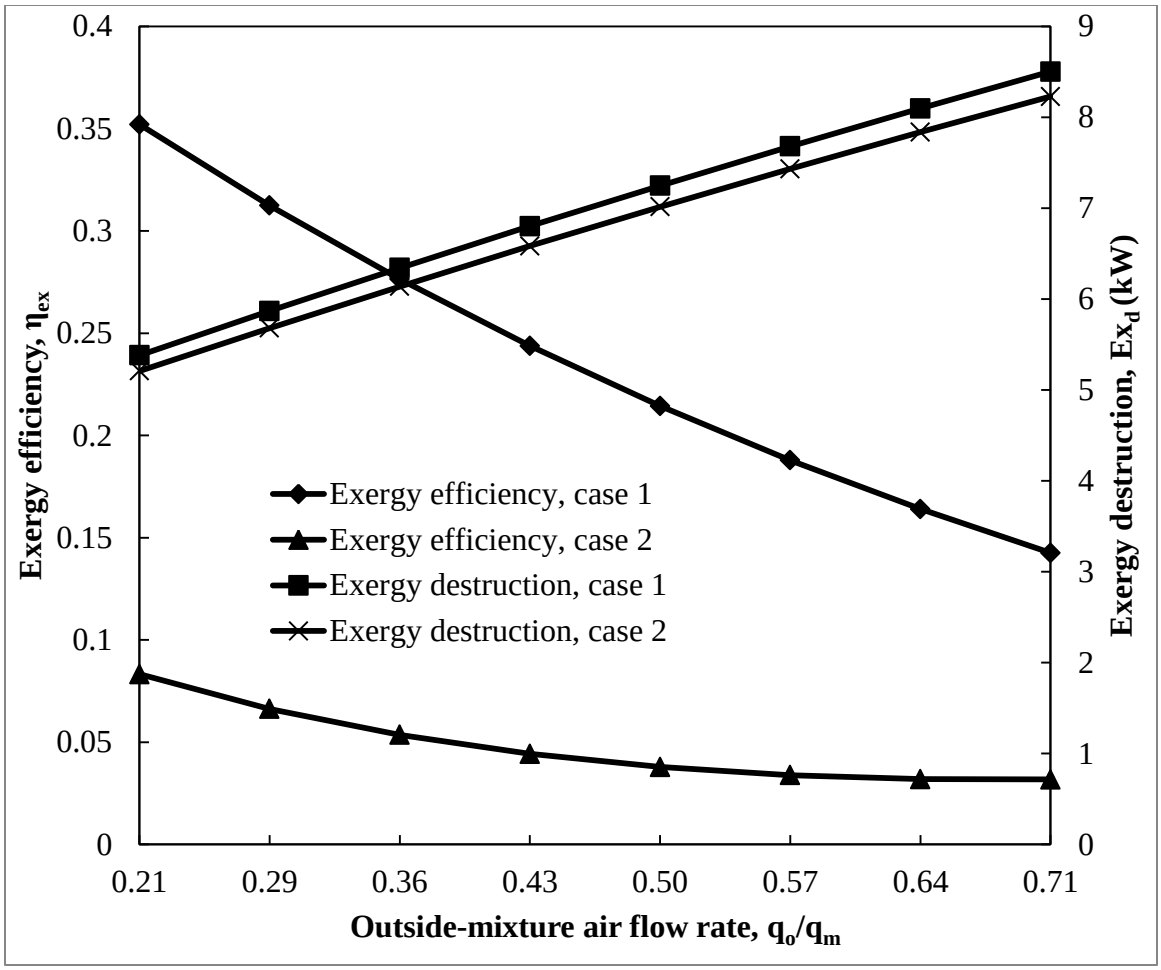

Figure 3.10: Effects of the outside-mixture air flow rate (q_o/q_m) on exergy efficiency and exergy destruction of the A/C system.

Chapter 4: Conclusions

4.1 Variable Refrigerant Flow

A number of important conclusions can be derived from the present numerical results. In this paper, the VRF system's performance was analyzed by varying different cycle parameters. The increment of the evaporator's temperatures increased the COP of the VRF cycle. The COP of the VRF system decreases as the condenser temperature of the system increases. The COP of the VRF system decreased more under different evaporator's temperature conditions. The COP of the VRF system decreased further for R-22 when evaporators are running at different temperatures. Part load calculations showed that the PLF decreases as the working load of the evaporators decrease. The simulation results compared reasonably well with the experimental data obtained from air conditioning manufacturer's catalogs [29, 30]. Present results showed a good agreement within an average percentage of error less than 10%. Many factors including the ideal assumptions affected the COP of the VRF system numerically studied; therefore, a percentage of error associated with the experimental results is expected.

4.2 Exergy

The simple air conditioning system has many factors that affect its performance. Our investigation showed that air conditioning systems have low exergy efficiency. Relationships between exergy efficiency, exergy destruction, and exergy input to

different parameters of psychrometric process have been studied thoroughly. Maximum exergy efficiency can be reached by increasing exergy input and decreasing exergy destruction of the A/C system. Exergy efficiency also can be increased by increasing exergy input by a higher rate than exergy destruction or by decreasing exergy destruction in a higher rate than exergy input. Large systems with multiple indoor units can be analyzed by using the same system of equations presented to calculate their exergy efficiency.

4.3 Recommendations for Future Research

Future work can be conducted for the VRF system by analyzing the effects of pressure drops in condenser and evaporators by taking into account the effects of heat transfer and friction in refrigerant pipes. Also, studying similar systems under heating or simultaneous cooling/heating conditions is substantial to improve the VRF system.

Moreover, future work can be done by analyzing exergy efficiency of A/C systems under heating condition. This kind of study will be more valuable for places where heating is used most of the year. Also, exergy analysis can be conducted for variable refrigerant flow systems since they are known for their high performance and energy savings. This will uncover any room for more improvement in such system.

References

[1] Stoeker, W.F., and Jones, J.W., *Refrigeration and air conditioning*, 2nd ed., McGraw-Hill, Inc., USA, 1982.

[2] Strand, R.K., Fisher, D.E., Liesen, R.J., and Pedersen, C.O., "Modular HVAC simulation and the future integration of alternative cooling systems in a new building energy simulation program", *ASHRAE Transactions*, vol. 108, no. 2, pp. 1107-1117, 2002.

[3] Xia, J., Winandy, E., Georges, B., and Lebrun, J., "Experimental analysis of the performances of variable refrigerant flow systems", *Building Sevr Eng Res Technol*, vol. 25, no. 1, pp. 17-23, 2004.

[4] Goetzler, W., "Variable refrigerant flow systems", *ASHRAE Journal*, April, 2007.

[5] Zhou, Y.P., Wu, J.Y., Wang, R.Z., and Shiochi, S., "Energy simulation in the variable refrigerant flow air-conditioning system under cooling conditions", *Energy and Buildings*, vol. 39, pp. 212-220, 2007.

[6] Zhou, Y.P., Wu, J.Y., Wang, R.Z., Shiochi, S., and Li, Y.M., "Simulation and experimental validation of the variable-refrigerant-volume (VRV) air-conditioning system in EnergyPlus", *Energy and Buildings*, vol. 40, pp. 1041-1047, 2008.

[7] Aynur, T.N., Hwang, Y., and Radermacher, R., "Simulation comparison of VAV and VRF air conditioning systems in an existing building for the cooling season", *Energy and Buildings*, vol. 41, pp. 1143-1150, 2009.

[8] Wang, X., Xia, J., Zhang, X., Shiochi, S., Peng, C., and Jiang, Y., "Modeling and experiment analysis of variable refrigerant flow air-conditioning systems", *Proceedings of International IBPSA Conference*, pp. 361-368, Glasgow, Scotland, 2009.

[9] Li, Y.M., Wu, J.Y., and Shiochi, S., "Experimental validation of the simulation module of the water-cooled variable refrigerant flow system under cooling operation", *Applied Energy*, vol. 87, pp. 1513-1521, 2010.

[10] Li, Y.M., and Wu, J.Y., "Energy simulation and analysis of the heat recovery variable refrigerant flow system in winter", *Energy and Buildings*, vol. 42, pp. 1093-1099, 2010.

[11] Bettanini, E., Gastaldello, A., and Schibuola, L., "Simplified models to simulate part load performances of air conditioning equipments", *Proceedings of International IBPSA Conference*, pp. 107-114, Eindhoven, Netherlands, 2003.

[12] Krakow, K.I., "Relationships between irreversibility, exergy destruction, and entropy generation for systems and components" *ASHRAE Transactions*, vol. 100, no. 1, pp. 3-10, 1994.

[13] Chengqin, R., Nianping, L., and Guangfa, T., "Principles of exergy analysis in HVAC and evaluation of evaporative cooling schemes", *Building and Environment*, vol. 37, pp. 1045-1055, 2002.

[14] Cervantes, J.G., and Torres-Reyes, E., "Experiments on a solar-assisted heat pump and an exergy analysis of the system", *Applied Thermal Engineering*, vol. 22, pp. 1289-1297, 2002.

[15] Bilgen, E., and Takahashi, H., "Exergy analysis and experimental study of heat pump systems", *Exergy, an International Journal*, vol. 2, pp. 259-265, 2002.

[16] Qureshi, B.A., and Zubair, S.M., "Application of exergy analysis to various psychrometric processes", *International Journal of Energy Research*, vol. 27, pp. 1079-1094, 2003.

[17] Utlu, Z., and Hepbasli, A., "A study on the evaluation of energy utilization efficiency in the Turkish residential-commercial sector using energy and exergy analyses", *Energy and Buildings*, vol. 35, pp. 1145-1153, 2003.

[18] Alpuche, M.G., Heard, C., Best, R., and Rojas, J., "Exergy analysis of air cooling systems in buildings in hot humid climates", *Applied Thermal Engineering*, vol. 25, pp. 507-517, 2005.

[19] Alhazmy, M.M., "Power estimation for air cooling and dehumidification using exergy analysis", *International Journal of Exergy*, vol. 3, no. 4, pp. 391-401, 2006.

[20] Rosen, M.A., Dincer, I., and Kanoglu, M., "Role of exergy in increasing efficiency and sustainability and reducing environmental impact", *Energy Policy*, vol. 36, pp. 128-137, 2008.

[21] Muangnoi, T., Asvapoositkul, W., and Wongwises, S., "Effects of inlet relative humidity and inlet temperature on the performance of counterflow wet cooling tower based on exergy analysis", *Energy Conversion and Management*, vol. 49, pp. 2795-2800, 2008.

[22] Wei, Z., and Zmeureanu, R., "Exergy analysis of variable air volume systems for an office building", *Energy Conversion and Management*, vol. 50, pp. 387-392, 2009.

[23] Ahmed, J.U., Saidur, R., and Masjuki, H.H., "A review on exergy analysis of vapor compression refrigeration system", *Renewable and Sustainable Energy Reviews*, vol. 15, pp. 1593-1600, 2010.

[24] Kanoglu, M., Dincer, I., and Rosen, M.A., "Exergy analysis of psychrometric processes for HVAC&R applications", *ASHRAE Transactions*, vol. 113, no. 2, pp. 172-180, 2007.

[25] Moran, M.J., Shapiro, H.N., Boettner, D.D., and Baily, M.B., *Fundamentals of engineering thermodynamics*, 7th ed., John Wiley & Sons, Inc., USA, 2011.

[26] CHEMCAD. Version 6.1.2: Process Flow Sheet Simulator. Chemstations Inc.: Houston, 2008.

[27] Edwards, J.E., *Process modeling selection of thermodynamic methods*, P & I Design Ltd., Process Instrumentation Consultancy & Design, 2008.

[28] Kim, J., Braun, J.E., and Groll, E.A., "A hybrid method for refrigerant flow balancing in multi-circuit evaporators: Upstream versus downstream flow control", *International Journal of Refrigeration*, vol. 32, pp. 1271-1282, 2009.

[29] Hitachi. Set-free fsn: variable refrigerant flow air conditioning systems (R410A), Hitachi Appliances Inc., Japan, 2008.

[30] Toshiba. VRF series: the most advanced commercial air conditioning system, Toshiba Carrier UK Ltd., UK, 2008.

[31] ASHRAE Handbook of Fundamentals, ASHRAE, Atlanta, Gorgia, USA, 2009.